Journal of Controlled Release 358 (2023) 171–189

Contents lists available at ScienceDirect

Journal of Controlled Release

journal homepage: www.elsevier.com/locate/jconrel

Escinosome thermosensitive gel optimizes efficacy of CAI-CORM in a rat model of rheumatoid arthritis

Giulia Vanti [a,1], Laura Micheli [b,1], Emanuela Berrino [c], Lorenzo Di Cesare Mannelli [b], Irene Bogani [a], Fabrizio Carta [c], Maria Camilla Bergonzi [a], Claudiu T. Supuran [c], Carla Ghelardini [b], Anna Rita Bilia [a,*]

[a] Department of Chemistry "Ugo Schiff" (DICUS), University of Florence, Via Ugo Schiff 6, 50019 Sesto Fiorentino, Firenze, Italy
[b] Pharmacology and Toxicology Section, Department of Neuroscience, Psychology, Drug Research and Child Health (NEUROFARBA), University of Florence, Viale G. Pieraccini 6, Firenze 50139, Italy
[c] Section of Pharmaceutical and Nutraceutical Sciences, Department of Neuroscience, Psychology, Drug Research and Child Health (NEUROFARBA), University of Florence, Via Ugo Schiff 6, 50019 Sesto Fiorentino, Firenze, Italy

ARTICLE INFO

Keywords:
CAI-CORM
Escinosome
Thermosensitive gel
Intra-articular administration
Rheumatoid arthritis
Pain

ABSTRACT

Rheumatoid arthritis is among the most common disabling diseases associated with chronic inflammation. The efficacy of the current therapeutic strategies is limited; therefore, new pharmacological agents and formulation approaches are urgently needed. In this work, we developed a thermosensitive gel incorporating escinosomes, innovative nanovesicles made of escin, stabilized with 10% of tween 20 and loaded with a Carbonic Anhydrase Inhibitor (CAI) bearing a Carbon Monoxide Releasing Moiety (CORM) (*i.e.*, CAI-CORM **1**), previously synthesized by some of the authors as a new potent pain-relieving agent. The light scattering analysis of the developed formulation showed optimal physical parameters, while the chromatographic analysis allowed the quantification of the encapsulation efficiency (90.1 ± 5.91 and 91.6 ± 8.46 for CAI-CORM **1** and escin, respectively). The thermosensitive gel, formulated using 23% *w/v* of poloxamer 407, had a sol-gel transition time of 40 s and good syringeability. Its stability in simulated synovial fluid (SSF) was morphologically evaluated by electron microscopy. Nanovesicles were physically stable in contact with the medium for two weeks, maintaining their original dimensions and spherical shape. The viscosity increased by about 30- to 100-fold with the temperature change from 25 °C to 37 °C. The gel erosion in SSF occurred within 9 h (88.2 ± 0.743%), and the drug's passive diffusion from escinosomes lasted 72 h, allowing a potential sustained therapeutic effect. The efficacy of a single intra-articular injection of the gel containing escinosomes loaded with CAI-CORM **1** (3 mg/mL; 30 μL, CAI-CORM **1** formulation) and the gel containing unloaded escinosomes (30 μL, blank formulation) was evaluated in a rat model of Complete Freund's Adjuvant (CFA)–induced rheumatoid arthritis. CAI-CORM **1** formulation was assessed to counteract mechanical hyperalgesia, spontaneous pain, and motor impairments on days 7 and 14 after treatment. The histological evaluation of the joints stressed the improvement of several morphological parameters in CFA + CAI-CORM **1** formulation-treated rats. In conclusion, the hybrid molecule CAI-CORM **1** formulated in escinosome-based thermosensitive gel could represent a new valid approach for managing rheumatoid arthritis.

1. Introduction

Rheumatoid arthritis is a chronic, inflammatory, autoimmune disease affecting joints with different severity among patients. Both cartilage and bone of joints are destroyed, and the tendons and ligaments become weaker with the progression of the disease [1]. These dramatic damages lead to chronic pain that negatively affects the patient's quality of life. Consequently, treatment for RA aims to decrease

* Corresponding author at: Department of Chemistry "Ugo Schiff", Via Ugo Schiff 6, 50019 Sesto Fiorentino, Firenze, Italy.
E-mail addresses: giulia.vanti@unifi.it (G. Vanti), laura.micheli@unifi.it (L. Micheli), emanuela.berrino@unifi.it (E. Berrino), lorenzo.mannelli@unifi.it (L.D.C. Mannelli), fabrizio.carta@unifi.it (F. Carta), mc.bergonzi@unifi.it (M.C. Bergonzi), claudiu.supuran@unifi.it (C.T. Supuran), carla.ghelardini@unifi.it (C. Ghelardini), ar.bilia@unifi.it (A.R. Bilia).
[1] These authors contributed equally

https://doi.org/10.1016/j.jconrel.2023.04.045
Received 8 November 2022; Received in revised form 18 April 2023; Accepted 27 April 2023
Available online 4 May 2023
0168-3659/© 2023 The Authors. Published by Elsevier B.V. This is an open access article under the CC BY license (http://creativecommons.org/licenses/by/4.0/).

pain, control joint inflammation, and reduce joint destruction and deformity, but regrettably, no current therapies are satisfactory and acceptable.

Conventional medications are principally nonsteroidal anti-inflammatory drugs (NSAIDs), including acetylsalicylate, ibuprofen, and naproxen. NSAIDs are associated with common side effects like nausea, ulcers, abdominal pain, and gastrointestinal bleeding after repeated use [2,3]. Corticosteroids are also prescribed because they are potent anti-inflammatory drugs, but they are indicated only for short treatment periods at the lowest possible doses to avoid the strong side effects (feasibly thinning of bones, weight gain, and diabetes) [4]. Currently, methotrexate and other conventional synthetic disease-modifying antirheumatic drugs such as leflunomide and sulfasalazine can be part of the treatment strategy. In contrast, the Janus kinase inhibitors (baricitinib, tofacitinib, and upadacitinib) and biological disease-modifying antirheumatic drugs are second-line treatments. However, these drugs present high percentages of treatment failure and are very expensive compared to NSAIDs and corticosteroids. Furthermore, conventional synthetic disease-modifying antirheumatic drugs can cause side effects, including liver damage and severe lung infections. Infections, the risk of blood clots in the lungs, serious heart-related events, and cancer can also be caused by Janus kinase inhibitors and biologics [5,6]. Hence, new pharmacological strategies based on innovative drugs and smart local drug delivery systems to retain drugs in the joint and reduce the dosing frequency are mandatory to improve rheumatoid arthritis clinical management.

Focusing our attention on the intra-articular therapy, mainly represented by lubricants or viscosifiers (principally hyaluronic acid) for the treatment of rheumatoid arthritis [7], this research aimed to investigate escinosomes embedded in a thermosensitive gel as an innovative formulation for intra-articular administration of a selected new generation of dual-acting molecules consisting of a Carbonic Anhydrase Inhibitor (CAI) of the sulfonamide type linked to a CO releasing-moiety (CORM) (CAI-CORMs). These new molecules have been synthesized to merge two therapeutically active portions within a single molecule endowed with anti-inflammatory and pain-relieving properties. Based on the di-cobalt-hexacarbonyl (DCH) moiety, the CORM portion ensured the release of CO, an endogenous gas-transmitter with cytoprotective and homeostatic features [8]. The administration of CO in the gaseous form or the CO released from a metallic-organic scaffold (CORM) has been widely explored so far, obtaining promising results in both *in vitro* and *in vivo* models of several inflammatory-based diseases, including rheumatoid arthritis [8–10]. On the other hand, the sulfonamide head portion was responsible for CAs inhibition. Beneficial effects in reliving rheumatoid arthritis ache symptoms have been observed when the CA isoforms (CA I, IV, IX, and XII) involved in the pathogenesis and maintenance of rheumatoid arthritis were inhibited [11,12]. Proof-of-concept studies using CAI-CORM hybrids have revealed that this association can successfully produce a synergistic anti-hyperalgesic effect in an *in vivo* rat model of rheumatoid arthritis [11].

Among the recently synthesized CAI-CORM hybrids, CAI-CORM **1** (Fig. 1) has been selected as the most promising because it inhibits the CA isoforms by producing a slow but sustained CO release over time in the Myoglobin (Mb) carbonylation assay. Furthermore, CAI-CORM **1** induces a higher pain-relieving effect when compared to the effects exerted by the CAI precursor and the CORM portion administered separately [11].

In a previous study, CAI-CORM **1** was orally administered as a suspension in a 1% solution of carboxymethyl cellulose sodium salt because of the low solubility in water media and its unfeasibility by intra-articular injection, reducing the overall systemic exposure.

The intra-articular drug delivery is one of the most effective treatments for arthritis. It can directly deliver the drug to the diseased joint site and increase the local drug concentration. Rapid onset, low side effects, and high patient tolerance are the main advantages of intra-articular-injected preparations [13,14]. However, intra-articular

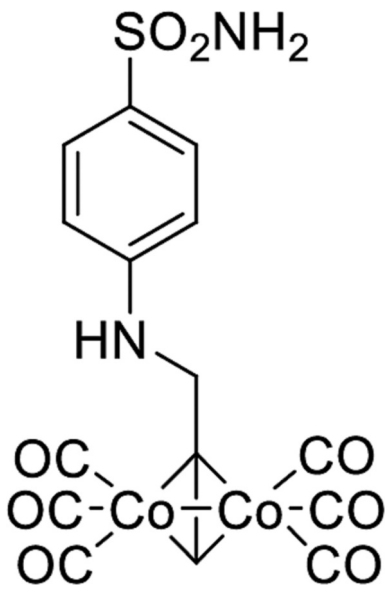

Fig. 1. Chemical structure of CAI-CORM **1**.

administration of conventional drug solutions or dispersions has a limited therapeutic effect because of the poor permeability of drugs into the cartilage and the relatively short retention time due to the rapid clearance from the joint by uptake into the synovial capillaries and lymphatics, particularly for small drug molecules. Special consideration should also be paid to the macrophage response to the injected materials, which leads to lowered drug concentration.

Therefore, various drug delivery systems for intra-articular injection, such as nanoparticles, liposomes, and gels, have been developed to increase the drug bioavailability in the joint cavity [14–16]. Nanocarriers can increase drug retention at the injection site, minimize the initial burst effect and provide a sustained release, reduce drug degradation, and, consequently, prolong the duration of action of the conveyed drug [14]. Furthermore, besides delivering therapeutic agents to joints with described advantages, intra-articular injection of phospholipid-based formulations provides a boundary lubrification of the cartilage thanks to the high hydration of the polar headgroups they expose, contributing positively to the treatment of rheumatoid arthritis [17,18]. At the same time, drug-incorporated hydrogels are much investigated for intra-articular administration because their high viscosity allows drug retention at the joint site, and their high-water content has a lubricating and soothing effect on the inflamed tissues, mimicking the soft tissues within the synovium. Of particular interest are *in situ* forming hydrogels, like thermosensitive hydrogels, that exhibit a sol-gel phase transition near body temperature. They are easily injected as solutions or suspensions but become gels after administration providing a depot for a slow and continuous release of the incorporated drug [14,17]. Accordingly, since nanoparticles and liposomes have the downside of being quickly cleared from the joint cavity or phagocytized by macrophages in synovial linings, although their capability of prolonging the retention time of the drug compared to conventional solutions or suspensions, drug-loaded nanocarriers embedded in thermosensitive hydrogels are gaining much attention because they can merge the advantages of both systems [13,14,19,20].

In this study, we developed and investigated a thermosensitive gel based on escinosomes loaded with CAI-CORM **1** for intra-articular admnistration. Escinosomes are deformable nanovesicles made of phosphatidylcholine (P90G) and escin (ESN), a bioactive triterpene saponin working as a vesicle bilayer component retaining ESN biological activities, and successfully reported for the delivery of drugs for dermal and subcutaneous administration [21,22]. Escinosomes loaded with CAI-CORM **1** were formulated in an *in situ* gelling and thermic-reversible

system, allowing a sustained drug release by forming a gel depot, avoiding repeated administrations, and improving patient compliance. The performance of the thermosensitive gel was investigated in a rat model of unilateral rheumatoid arthritis induced by Complete Freund's Adjuvant (CFA) intra-articular injection [23,24]. CAI-CORM **1**-loaded escinosomes were physically characterized by light scattering techniques and electron microscopy in terms of Size, PdI, ζ-potential and morphology, and chemically evaluated regarding recovery and encapsulation efficiency of CAI-CORM **1** and ESN. The stability of CAI-CORM **1** in escinosomes and the thermosensitive gel formulation was assessed by HPLC-MS. The thermosensitive formulation loaded with CAI-CORM **1** was also evaluated for stability in simulated synovial fluid and the *in vitro* release. *In vivo* studies were carried out to investigate the anti-hyperalgesic effects of a single intra-articular injection of the developed thermosensitive gel loaded with CAI-CORM **1** in a rat model of CFA–induced rheumatoid arthritis. Moreover, the protective effect of the treatments was analyzed by the histological evaluation of the joint tissues.

2. Materials and methods

2.1. Chemicals

Anhydrous solvents and all reagents were purchased from Sigma-Aldrich (Milan, Italy), Alfa Aesar (Milan, Italy), and TCI (Milan, Italy). All reactions involving air- or moisture-sensitive compounds were performed under a nitrogen atmosphere using dried glassware and syringe techniques to transfer solutions. Nuclear magnetic resonance spectra (^{1}H NMR: 400 MHz; ^{13}C NMR: 100 MHz) were recorded in DMSO-d_6 using an AVANCE III 400 MHz spectrometer (Bruker, Milan, Italy). Chemical shifts are reported in parts per million (ppm), and the coupling constants (*J*) are expressed in hertz (Hz). Splitting patterns are designated as follows: s, singlet; d, doublet; t, triplet; q, quadruplet; m, multiplet; brs, broad singlet; and dd, double of doublets. The addition of D_2O confirmed the exchangeable protons (OH and NH) assignment. Analytical thin-layer chromatography (TLC) was carried out on silica gel F-254 plates (Merck, Milan, Italy). Phosphatidylcholine (Phospholipon 90G, P90G) was purchased from Lipoid AG (Cologne, Germany) with the support of the Italian agency AVG Srl. Cholesterol 95%, escin (ESN), bovine serum albumin (BSA), poloxamer 407, Tween 20, phosphate buffer saline (PBS), dichloromethane, methanol, ammonium acetate, LC-MS grade water, LC-MS grade acetonitrile, and all HPLC grade solvents (acetonitrile, methanol, formic acid) were bought from Merck Life Science Srl (Milano, Italy). Vegetable glycerol Eur Ph. and propylene glycol Eur Ph. were from Galeno Srl (Prato, Italy). Powder soy lecithin was purchased from Acef Spa (Piacenza; Italy), and 0.9% sodium chloride physiological solution was from Eurospital Spa (Trieste, Italy). Phosphotungstic acid was acquired from Electron Microscopy Sciences (Hatfield, PA, USA), and injectable sodium hyaluronate (molecular weight range from 3000 to 40,000 KDa) was purchased from Altergon Italia Srl. Ultrapure water was produced by a synergy UV Simplicity water purification system provided by Merck Life Science Srl (Milano, Italy).

2.2. Synthesis of CAI-CORM 1

CAI-CORM **1** was synthesized, purified, and characterized as previously reported [11]. The alkyne precursor 4-(Prop-2-ynylamino)benzenesulfonamide (0.1 g, 1.0 equiv) was dissolved in tetrahydrofuran (THF, 5 mL), and then dicobalt octacarbonyl (1.05 equiv) was added. The black mixture was stirred at r.t. for 40 min (TLC monitoring). Then, SiO_2 was added, and the solvent was removed under vacuum to give a black solid residue. The crude product was purified by silica gel column chromatography eluting with 40% ethyl acetate in *n*-hexane to afford the desired product as a red solid. **4-(Prop-2-ynylamino)benzenesulfonamidehexacarbonyldicobalt** (CAI-CORM **1**): 42% yield; silica gel TLC Rf = 0.54 (EtOAc/*n*-Hex 60% *v*/v). δ_H (400 MHz, DMSO-d_6) 4.60 (2H, s, CH_2), 6.69 (1H, s, C*H*), 6.71 (2H, d, *J* = 8.5, Ar—*H*), 7.00 (2H, br s, exchange with D_2O, SO_2NH_2), 7.16 (1H, m, exchange with D_2O, N*H*), 7.57 (2H, d, *J* = 8.5, Ar—*H*); δ_C (100 MHz, DMSO-d_6) 44.3, 74.1, 94.3, 111.1, 127.3, 130.7, 150.1, 199.9; *m/z* (ESI negative), 495.88 $[M + H]^-$ [11].

2.3. HPLC-DAD analysis for the quantification of CAI-CORM 1 and ESN

Quantitative determination of CAI-CORM **1** and ESN was carried out using an 1100 High-Performance Liquid Chromatograph (HPLC) equipped with a Diode Array Detector (DAD) (Agilent Technologies Italia Spa; Rome, Italy) and an Eclipse XDB-C18 column with an internal diameter of 3.5 μm and (150 × 4.6) mm dimensions. The analyses were performed using a mobile phase composed of (A) formic acid/water (pH 3.2) and (B) acetonitrile with a 0.6 mL/min flow rate and the following multi-step gradient: 0–20 min 20–100% B; 20–25 min 100% B; 25–35 min 100–20%; post time was 5 min. The temperature was set at 25 °C. UV–visible spectra were recorded in the 200–600 nm range, and chromatograms were acquired at 210 nm for ESN and 274 nm for CAI-CORM **1**. The calibration curves were prepared by solubilizing CAI-CORM **1** in acetonitrile at 0.2 mg/mL and ESN in methanol at 5 mg/mL. A linear relationship was obtained in the investigated concentration range of 3000–1 ng for CAI-CORM **1** (R^2 = 0.9999) and 50,000–125 ng for ESN (R^2 = 0.9999).

2.4. HPLC-UV-ESI MS analysis to assess the stability of CAI-CORM 1

The analyses were carried out by high-performance liquid chromatography-ultraviolet detector-electrospray mass spectrometry (HPLC-UV-ESI MS) using a Waters instrument (Waters Italy, Sesto S. Giovanni, Milan, Italy). The apparatus consisted of an Alliance 2695 HPLC with an autosampler, a column oven, and a DAD 2996 coupled in series to a Quattro micro triple quadrupole mass spectrometer equipped with a *Z*-spray ESI interface.

The LC column was a Gemini C18, 100 × 2 mm, 5 μm (Phenomenex Italia, Bologna, Italy), and the separation was performed using gradient elution with the following program: 0–15 min 85%–10% A, 15–20 min 10% A. The eluent A was ammonium acetate 5 mM pH 4, and the eluent B was acetonitrile. The flow rate was set at 0.3 mL/min, and the column temperature was at 30 °C. The injection volume was 25 μL, and no splitter was used between UV and MS detectors. UV spectra were recorded in the range 205–350 nm at 2.4 nm resolution and 1 spectrum/s rate. ESI interface and MS parameters were optimized during the infusion of the analyte solution. Specifically, they were: spray capillary 3.9 kV, cone voltage 6 V, extractor lens 3 V, source temperature 120 °C, and desolvation gas temperature 320 °C. High-purity nitrogen (N_2) was used as cone gas and desolvation gas at 21 L/h and 400 L/h, respectively. The mass spectrometer operated in positive ion mode, and data were acquired in full scan in the *m/z* range from 290 to 1180 at 0.5 s scan time.

Before the analysis, CAI-CORM **1**-loaded escinosomes were diluted 200-fold in acetonitrile to break the vesicle bilayer and solubilize the active substances. Samples were vortexed for 30 s, sonicated in the ultrasonic bath for 15 min at 25 °C, and centrifuged at 16873 ×*g* using the Centrifuge 5418 R (Eppendorf Srl; Milano, Italy) for 10 min. The supernatants were analyzed by HPLC-UV-ESI MS.

2.5. Preparation of escinosomes

The escinosomes were prepared using the thin-layer evaporation method. Different gravimetric ratios (5:1, 4:1, 3:1, 2:1) of P90G and ESN were tested, keeping fixed ESN concentration at 5 mg/mL and changing P90G concentration (25, 20, 15, and 10 mg/mL), according to previous studies [21,22]. P90G and ESN were dissolved in dichloromethane and methanol (1:1 volumetric ratio), improving the solubilization with the

ultrasonic bath for 1 min. The organic solvents were removed by a rotavapor coupled to a membrane pump under reduced pressure at 30 °C for 20 min. The lipid film obtained was hydrated with 5 mL of a physiological solution under mechanical stirring at 700 rpm for 30 min, immersing the flask in the ultrasonic bath. During the hydration step, the bathwater temperature increased from approximately 18 °C to 32 °C.

2.6. Preparation of CAI-CORM 1-loaded escinosomes

Escinosomes loaded with CAI-CORM **1** (3 mg/mL) were prepared as described in paragraph 2.5 using the selected combination (gravimetric ratio 5:1) of P90G and ESN and solubilizing the lipophilic CAI-CORM **1** in the organic solvents. Different hydration mediums and times were tested, and other techniques were applied to reduce the nanovesicles' PdI and develop the final formulation. This optimization was carried out using extrusion or ultrasonication or modifying the composition of the hydration medium.

2.6.1. Extrusion procedure

CAI-CORM **1**-loaded escinosomes, prepared as described in paragraph 2.6, were optimized by extrusion using the LipoFast-Basic extruder (Avestin Europe GmbH; Mannheim, Germany). The extrusion forces vesicles through tiny pores to reduce their dimensions and polydispersity [25,26]. The formulation was extruded, performing a different number of passages (*i.e.*, 11, 21, 31, 51) through 19 mm polycarbonate membranes (Avestin Europe GmbH; Mannheim, Germany) with different pore sizes (namely 50, 100, 200, 400 nm) at the constant pressure of 7 bar. Specifically, 1 mL of the formulation was placed in a syringe, and the obtained extruded sample was collected in a second receiving syringe.

2.6.2. Ultrasonication procedure

CAI-CORM **1**-loaded escinosomes were also optimized by ultrasonication using the Sonopuls Ultrasonic Homogenizer HD 2200 by Bandelin electronic GmbH & Co. KG (Berlin, Germany) coupled with the MS 72 probe [21]. Different times (1, 5, 10, 15 min) and cycles (1, 2, 3 tenths of a second) of sonication, with a constant amplitude of 48%, were applied to reduce vesicle size and increase sample homogeneity. The formulation was placed in an ice bath during the sonication to avoid excessive warm-up.

2.6.3. Addition of polyols or surfactants to escinosomes

Escinosome polydispersity was also improved by adding polyols (glycerol or propylene glycol) or surfactants (Tween 20) [27–29]. CAI-CORM **1**-loaded escinosomes were prepared as described in paragraph 2.6 using mixtures of physiological solution and glycerol or propylene glycol or Tween 20 at two different concentrations (5, 10% *v*/v). The lipid film hydration was carried out in one step, adding 5 mL of hydration medium and mechanically stirring for 30 min, or in two steps, adding 2.5 mL of solution and stirring for 30 min and subsequently adding 2.5 mL more and stirring for further 30 min [30]. The obtained escinosomes were left to stabilize at 4 °C in the fridge for one night.

2.7. Preparation of the thermosensitive gel based on CAI-CORM 1-loaded escinosomes

A thermosensitive gel incorporating CAI-CORM **1**-loaded escinosomes was prepared by adding poloxamer 407 powder to CAI-CORM **1**-loaded escinosomes, previously prepared according to the method described in paragraph 2.6.3. Different percentages of poloxamer 407, ranging from 12 to 25% *w/v*, were tested [31] by solubilization in CAI-CORM **1**-loaded escinosomes under magnetic stirring for 24 h at 300 rpm at room temperature (25 °C). Specifically, the final thermosensitive gel, used for all subsequent *in vitro* and *in vivo* studies, was obtained by dissolving 23% w/v of poloxamer 407 in CAI-CORM **1**-loaded escinosomes by magnetic stirring for 24 h at 300 rpm at room temperature (25 °C). The proper percentage of poloxamer 407 was selected based on the sol-gel transition time and syringeability.

2.8. Sol-gel transition time and syringeability

The sol-gel transition time was evaluated for the developed thermosensitive gel using the test tube inverting method [32]. A glass test tube was filled with about 0.5 mL of sample in the sol form and immersed in water at the exact and controlled temperature of 37 °C. The time the formulation took to pass from liquid to gel was considered the gelation time. The occurred gelation was verified by turning the tube when the meniscus would no longer move upon tilting at a 90° angle. The syringeability was assessed qualitatively [32]. A 1 mL syringe with a 26-gauge needle was filled with the formulation, applying a gentle and uniform force by pressing the syringe's injector part and avoiding forming air bubbles.

2.9. Physical and chemical characterization of formulations

2.9.1. Light scattering: DLS and ELS

Escinosomes were physically characterized by the light scattering technique to determine nanovesicles' average hydrodynamic diameter (Size, nm), polydispersity index (PdI, dimensionless measurement), and ζ-potential (mV) [21]. Dynamic and electrophoretic light scattering (DLS-ELS) analysis was performed using the Zetasizer Nanoseries ZS90, equipped with a 4 mW He—Ne laser, operating at 632.8 nm, and an APD detector (Malvern instrument; Worcestershire, UK). Time correlation functions were analyzed using the software Zetasizer, version 7.02, provided by Malvern, and all data were processed using the Cumulants method defined in the International Standards ISO22412 (2008) and recognized by Health Agencies [33–35]. This method allows for determining Size and PdI. Measurements were carried out in triplicate at (25 ± 2)°C and a scattering angle of 90°. The formulation was analyzed after 100-fold dilution in ultrapure water using square polystyrene cuvettes for DLS and folded capillary zeta cells for ELS.

2.9.2. Electron microscopy: TEM and STEM

CAI-CORM **1**-loaded escinosomes and the corresponding thermosensitive gel were morphologically characterized by transmission electron microscopy (TEM) on a TEM CM12 PHILIPS equipped with an OLYMPUS Megaview G2 camera [21]. Samples were analyzed at an accelerating voltage of 80 keV. The formulation was placed on a carbon film-covered copper grid. The sample excess was blotted from the grid with filter paper to obtain a thin film stained with a phosphotungstic acid solution (1% *w/v*) in distilled water. The analysis was performed 3 min after the staining.

Escinosomes were also analyzed by the scanning electron microscope Gaia 3 (Tescan s.r.o, Brno, Czech Republic), FIB-SEM (focused ion beam scanning electron microscope), operating in high-vacuum mode with electron beam voltage of 20 kV and bright-field transmission electron microscope detector. Gaia 3 was equipped with an EDS-X-ray microanalysis system (EDAX, AME- TEK, USA) TEAM EDS Basic Software Suite TEAM™ and was delivered with a STEM (scanning transmission electron microscopy) detector, which provides a complementary method for image acquisition of transmitted electrons. The detector consists of several semi-conductor sensors for bright and dark field imaging. The transmitted electron signal can be collected by placing the detection system below the specimen. The instruments are located in a room at a controlled temperature of 19 °C.

2.9.3. Recovery and encapsulation efficiency of ESN and CAI-CORM 1

Chemical characterization of CAI-CORM **1**-loaded escinosomes was conducted by measuring encapsulation efficiency (EE%) and recovery (R%) of CAI-CORM **1** and ESN. To determine EE%, the not encapsulated drugs were removed by the dialysis bag method, utilizing Spectra/Por® regenerated cellulose membranes, with 12–14 kDa molecular weight

cut-off, by Repligen Europe B.V. (Breda, The Netherlands) [30]. The dialysis bag with 1 mL of the formulation was submerged in 1 L of ultrapure water at (25 ± 1)°C and magnetically stirred at 100 rpm for 1 h. The purified formulation was then diluted in organic solvents to break the vesicle bilayer and solubilize the active substances. Specifically, the formulation was diluted 20-fold in methanol to determine ESN content and 200-fold in acetonitrile to determine CAI-CORM **1**. Samples were vortexed for 30 s, sonicated in the ultrasonic bath for 15 min at 25 °C, and centrifuged at 16873 ×*g* for 10 min. The supernatants were analyzed by HPLC-DAD. Similarly, R% was determined using the same procedure without dialysis and analyzing samples by HPLC-DAD. EE% and R% were calculated as the percentages of the concentrations determined by HPLC-DAD analysis, divided by the initial drug concentration determined by weighting, as previously reported.

2.10. Thermosensitive gel stability in simulated synovial fluid

The gel stability in simulated synovial fluid (SSF) was carried out for two weeks, according to the *in vivo* studies [36]. SSF was prepared by solubilizing 3 g/L sodium hyaluronate (HA), 19 g/L bovine serum albumin (BSA), 11 g/L IgG, and 0.1 g/L phospholipid lecithin in PBS 0.01 M pH 7.4 (containing 29 mM NaCl, 2.5 mM KCl, 7.4 mM $Na_2HPO_4 \bullet 7H_2O$, 1.3 mM KH_2PO_4) [37]. Precisely, the components were solubilized one by one, stirring at 100 rpm for 15 min after each addition. Then, the IgGs were added, and the final solution was stirred for a further 10 min. The thermosensitive gel was diluted in SSF in a 1:1 volumetric ratio, considering the injection volume (30 μL) during the *in vivo* studies and the tibio-tarsal fluid volume (30 μL) estimated in previous studies focused on managing articular pain by intra-articular treatment. These findings, attained by some of the authors, confirmed literature data highlighting that the rat's synovial fluid volume ranges from 10 to 100 μL [38]. The mixture was vortexed for 2 min and incubated in a Biosan PST-60HL thermo-shaker (Riga, Latvia) at the controlled temperature of 37 °C, far from the light, and under a horizontal mechanical stirring of 300 rpm. Gel physical stability was evaluated by TEM, as described in paragraph 2.9.2. The analysis was performed at the beginning of the study, after mixing the gel and SSF, and at the end, elapsed two weeks. Eventual color changes and precipitation processes were also visually assessed.

2.11. Viscosity test

The viscosity (mPa × s) of the thermosensitive gel based on CAI-CORM **1**-loaded escinosomes was measured at the controlled temperatures of (25 ± 1)°C and (37 ± 1)°C by a Brookfield DVE-RV digital viscometer (Ametek Brookfield; Milan, Italy), using the 03 and 07 spindles [39], selected by the "trial and error" method, because able to provide on-scale readings (% Torque between 10 and 100) with the highest number of the possible speeds [40]. The measurements were performed using about 60 g of sample. Two minutes were selected as spindle rotation time (time required for the viscosity reading to reach a constant value) for each tested rotational speed (1, 5, 10, 30, 50, and 100 rpm). Every 2 min, the rotational speed was increased (up viscosity ramp); then, every 2 min, the rotational speed was decreased (down viscosity ramp). All the viscosity measurements were recorded and plotted on a graph as a function of the spindle rotational speed. Temperature uniformity of the sample and spindle was ensured by immersing the beaker in a thermostatic water bath with a temperature probe and rotating the spindle inside the sample for 30 min before starting each measurement.

2.12. Drug release study from the thermosensitive gel based on CAI-CORM 1-loaded escinosomes

2.12.1. Thermosensitive gel erosion

The gel erosion or dissolution was investigated by the gravimetric method using the membrane-less model to allow direct contact between the gel and SSF [41–43]. Briefly, 500 mg of the thermosensitive gel incorporating CAI-CORM **1** escinosomes were weighted in an Eppendorf tube and placed in a water bath at 37 °C until gel formed. The SSF, prepared as described in paragraph 2.10, was pre-equilibrated in a water bath at 37 °C and carefully layered over the gel surface. Then, the Eppendorf tube was placed again in the water bath at 37 °C under magnetic stirring at 100 rpm for 10 h. Every hour, the SSF was removed entirely. The weight of the Eppendorf tube with the remaining gel was recorded. Hence, the tube with gel was warmed again in the water bath for about 45 s to ensure the semisolid state was maintained, and the previously removed SSF was replaced with the fresh medium. The experiment was carried out until the weight of the remaining gel was <10% of its initial weight [42]. The percentage of gel dissolved was calculated for each time point. A cumulative erosion rate curve was constructed by plotting the cumulative erosion rate on the y-axis and time on the x-axis.

2.12.2. Passive diffusion of CAI-CORM 1 and ESN from escinosomes

The release of CAI-CORM **1** and ESN from escinosomes was evaluated using the dialysis bag method [21]. The thermosensitive gel (1 mL) was mixed with SSF (prepared as described in paragraph 2.10) in a 1:1 volumetric ratio to simulate the *in vivo* dilution occurring after intra-articular administration and dissolution in the synovial fluid [38]. The mixture was put inside a Spectra/Por® dialysis tubing of regenerated cellulose with selective permeability and molecular weight cut-off of 12–14 kDa (Repligen Europe BV; Breda, The Netherlands). The bag was maintained under magnetic stirring at 100 rpm for 72 h in 100 mL of 10% *v*/v Tween 20/PBS warmed at (37 ± 1)°C controlled by a temperature sensor [22]. The acceptor medium (500 μL) was collected and replaced by an equal volume of the fresh medium at specific time points within 72 h. All withdrawn samples were analyzed by HPLC-DAD. The amount (R%) of ESN and CAI-CORM **1** that remained inside the bag was also determined after 8, 24, 48, and 72 h following the procedure described in paragraph 2.9.3 and applying a 10-fold dilution.

2.13. In vivo experiments

2.13.1. Animals

Sprague Dawley rats (Envigo, Varese, Italy) weighing 220–250 g at the beginning of the experimental procedure were used. Animals were housed in the Centro Stabulazione Animali da Laboratorio (University of Florence) and used at least one week after arrival. Four rats were housed per cage (size 26 cm × 41 cm); animals were fed with a standard laboratory diet and tap water *ad libitum* and kept at (23 ± 1)°C with a 12 h light/dark cycle (light at 7 A.M.). Formal approval to conduct the experiments described was obtained from the Italian Ministry of Health (No. 517/2017, 06/04/2017) and the Animal Subjects Review Board of the University of Florence.

2.13.2. Complete Freund Adjuvant–induced rheumatoid arthritis

Articular damage was induced by the injection of complete Freund's adjuvant (CFA; Sigma-Aldrich, Milan, Italy) into the tibiotarsal joint [23,24]. Briefly, the rats were lightly anesthetized with 2% isoflurane; the left leg skin was sterilized with 75% ethyl alcohol, and the lateral malleolus was located by palpation; then, a 28-gauge needle was inserted vertically to penetrate the skin and turned distally for insertion into the articular cavity at the gap between the tibiofibular and tarsal bone until a distinct loss of resistance was felt. A volume of 50 μL of CFA was then injected (day −7). Control rats received 50 μL of saline solution (day −7) in the tibiotarsal joint.

2.13.3. Intra-articular treatment with escinosomes

Thirty μL of CAI-CORM **1** formulation (thermosensitive gel of CAI-CORM **1**-loaded escinosomes; 3 mg/mL) or blank formulation (thermosensitive gel of unloaded escinosomes) were intra-articularly injected

on day 0, one week after the damage evoked by CFA. Behavioral measurements were performed 7 and 14 days after treatments with CAI-CORM **1** formulation or blank formulation [44].

2.13.4. Paw pressure test

The nociceptive threshold in the rat was determined with an analgesimeter (Ugo Basile, Varese, Italy), according to the method described by Leighton and coworkers [45]. Briefly, a constantly increased pressure was applied to a small area of the dorsal surface of the hind paw using a blunt conical mechanical probe. Mechanical pressure was increased until vocalization or a withdrawal reflex occurred while rats were lightly restrained. Vocalization or withdrawal reflex thresholds were expressed in grams. Rats scoring below 40 g or over 75 g during the test before drug administration (25%) were rejected. An arbitrary cut-off value of 100 g was adopted. The data were collected by an observer who was blinded to the protocol.

2.13.5. Incapacitance test

Weight-bearing changes were measured using the Incapacitance apparatus (Linton Instrumentation, Norfolk, UK) to detect changes in postural equilibrium after a hind limb injury [46]. Rats were trained to stand on their hind paws in a box with an inclined plane (65° from horizontal). This box was placed above the Incapacitance apparatus, allowing us to independently measure the weight the animal applied on each hind limb. The value reported for each animal is the mean of five consecutive measurements. In the absence of hind limb injury, rats applied equal weight on both hind limbs, indicating postural equilibrium. In contrast, an unequal weight distribution on the hind limbs showed a monolateral decreased pain threshold [46]. Data are expressed as the difference between the weight applied to the limb contralateral to the injury and the weight applied to the ipsilateral one (Δ weight).

2.13.6. von Frey test

The animals were placed in 20 × 20 cm plexiglass boxes equipped with a metallic meshy floor, 20 cm above the bench. A habituation of 15 min was allowed before the test. An electronic von Frey hair unit (Ugo Basile, Varese, Italy) was used: the withdrawal threshold was evaluated by applying force ranging from 0 to 50 g with a 0.2 g accuracy. Punctuate stimulus was delivered to the mid-plantar area of each anterior paw from below the meshy floor through a plastic tip, and the withdrawal threshold was automatically displayed on the screen. The paw sensitivity threshold was defined as the minimum pressure required to elicit a robust and immediate withdrawal reflex of the paw. Voluntary movements associated with locomotion were not taken as a withdrawal response. Stimuli were applied on each anterior paw with an interval of 5 s. The measure was repeated 5 times, and the final value was obtained by averaging the 5 measures [47].

2.13.7. Beam Balance test

A balance beam test [48] consisted of the rats being placed on a narrow strip of wood (30 cm × 1.3 cm) while balancing, and the scoring standards were as follows: 0 points, the four limbs were all on the wood in a balance situation; 1 point, limbs of one side were able to grasp the wood or shake on the wood; 2 points, one or two limbs slipped from the wood; 3 points, three limbs slipped from the wood; 4 points, suspended on the wood and fell over after struggle [49].

2.13.8. Histological evaluations

On day 14, after the behavioral measurements, the animals were sacrificed by decapitation, and the legs were collected and fixed in 4% formaldehyde in phosphate-buffered saline (PBS) for 48 h at room temperature for the histological studies. The samples were then decalcified using a 0.76 M sodium formate and 1.6 M formic acid solution in water for 4 weeks. The solution was changed every 7 days. The histological samples were firstly dehydrated in alcohol and then embedded in paraffin. Six μM sections of the tibiotarsal joint were hematoxylin and eosin stained and qualitatively blindly analyzed by two independent observers attributing a histological score as follows: (0: absent; 1: mild; 2: moderate; 3: severe) following these morphological parameters: (a) inflammatory infiltrate; (b) synovial hyperplasia; (c) fibrin deposition; (d) synovial vascularity; (e) cartilage erosion; (f) bone erosion; (g) joint space [50].

2.14. Statistical analysis

The researchers were blind to all treatments. The reported values represent the mean ± SEM of six rats per group, performed in two different experimental sets. The examination of variance was performed by an ANOVA. A Bonferroni's significant difference procedure was used as a post-hoc comparison. *P*-values of <0.05 were considered significant. Data were analyzed using Origin 9 software (OriginLab, Northampton, MA, USA).

3. Results and discussion

3.1. Preparation and characterization of escinosomes

Escinosomes are highly deformable vesicles, made of P90G and ESN, which preserve the anti-hyaluronidase activity of the saponin [21]. The safety profile of these excipients for intra-articular injection has already been studied [51–54]. Biodegradability is, in fact, a major concern in the choice of drug delivery vehicles for successful intra-articular treatment. Residual degradation products remaining within the joint may induce side effects such as inflammation [55]. Therefore, an ideal drug delivery system for arthritis treatment would be desirable to have excipients and related degradation products with exquisite biocompatibility to ensure the security of drug delivery [56]. In this study, escinosomes were developed to formulate the lipophilic active compound CAI-CORM **1**. First, empty escinosomes were prepared by testing different gravimetric ratios between P90G and ESN to reduce the excipient (P90G) concentration as much as possible, compared to the previously developed escinosomes [14,15] and keeping the nanosystem stable. The suitability of the dimensions and polydispersity of nanovesicles for the administration route at issue represent a priority aspect in formulation studies. Still, the intra-articular route offers a wide dimension range. Many authors reported on nanovectors with dimensions ranging from about 30 nm to several μm, suitable for intra-articular injection [57,58]. However, the pharmacokinetics of nanovectors within cartilage depends on their chemical and physical properties, including size, charge, surface chemistry, and the pathological state of the joint cavity [16,59,60].

Prepared escinosomes were analyzed by DLS and ELS to measure Size, PdI, and ζ-potential (Table 1). The P90G/ESN gravimetric ratio of 5:1 was selected because of smaller sizes, low PdI, and homogeneity of the obtained formulation. Also, no aggregation or sedimentation was observed by visual inspection. By contrast, the 4:1 gravimetric ratio was discarded because of the higher PdI. The formulations with a 3:1 and 2:1 gravimetric ratio were not uniform. Some aggregates formed quickly (Fig. 1 of Supplementary Material), despite having statistically higher ζ-potential in absolute value than the formulation with a 5:1 ratio and the formulation with a 2:1 ratio having an optimum PdI. The average size of selected escinosomes was about 164 nm (Table 1).

As the pore size of collagen type II fibrillar network is approximately

Table 1
Characterization of empty escinosomes. Results are shown as mean ± SD ($n = 3$).

P90G/ESN gravimetric ratio	Size (nm)	PdI	Z-potential (mV)
5:1	164 ± 1.30	0.249 ± 0.00473	−18.3 ± 0.233
4:1	240 ± 6.27	0.397 ± 0.00696	−32.6 ± 0.491^
3:1	212 ± 1.57	0.274 ± 0.00467	−26.1 ± 0.318^
2:1	222 ± 2.54	0.177 ± 0.0162	−22.7 ± 0.463^

^ = $P < 0.01$ *vs* 5:1 ratio.

50–60 nm in the superficial zone of human knee articular cartilage, nanovectors beyond this size may not be able to enter the cartilage matrix efficiently, and those larger than 1 μm are phagocytosed by the synovial macrophages [16,57,59,60]. On the other hand, larger-sized nanovectors show more retention upon local injection, while small-sized nanovectors may be quickly cleared from the joint *via* synovial capillaries and the lymphatic system or [16,59,60]. For this reason, optimal sizes of nanovesicles to maximize therapeutic efficacy are not easily predictable [57]. As this study aimed to obtain a drug depot in the joint cavity, developed escinosomes were found suitable for this purpose.

3.2. Preparation and characterization of CAI-CORM 1-loaded escinosomes

Escinosomes loaded with CAI-CORM **1** (3 mg/mL) were prepared using the P90G/ESN gravimetric ratio of 5:1 (25 and 5 mg/mL, respectively) and solubilizing CAI-CORM **1** in the mixture of dichloromethane and methanol. CAI-CORM **1** concentration was selected based on the injection volume used during the *in vivo* tests (30 μL) and the drug concentration used in previous studies by intra-articular injection for the local treatment of rheumatoid arthritis [44]. CAI-CORM **1**-loaded escinosomes were homogenized in size distribution using different approaches, including extrusion, ultrasonication, and stabilization by adding polyols or surfactants. All the obtained escinosomes were analyzed by DLS to measure Size and PdI. The first applied optimization method was extrusion, which only induced mechanical stress to the vesicles. The extrusion forces vesicles through tiny pores to reduce their dimensions and polydispersity [25,26]. The formulation was extruded using polycarbonate membranes with 400 and 200 nm pores and performing different passages (11, 21, 31, 51) (Table 2). Membranes with 400 nm pores gave the lowest PdI after 31 passages, and this value has been selected for further combination with 200 nm pores membranes. However, both 400 nm and 200 nm pore membranes and their combination were inefficient in obtaining homogeneous samples because PdI was always above 0.3 (Table 2). In addition, CAI-CORM **1** R%, determined for the formulation with the lowest PdI, obtained with 31 passages through 400 nm membranes and 31 passages through 200 nm membranes, was found to be 68.6 ± 0.964%. This result showed that CAI-CORM **1** concentration was affected by the extrusion process. Therefore, tested extrusion conditions could not homogenize the vesicles and reduce the active component's concentration.

Then, ultrasonication was carried out as an alternative optimization method. Specifically, different cycles (1,2,3) and times (5, 10) of sonication were applied (Table 3). The best results in terms of polydispersity were obtained with 3 cycles for 10 min because the PdI was 0.260 ± 0.0180 (Table 3).

Lastly, a different technique was adopted to achieve a homogeneous formulation. Polyols (glycerol and propylene glycol) or surfactants (Tween 20) were added to the hydration medium in different percentages (5, 10% *v*/v) to stabilize the vesicle bilayer (Table 4) [27,28]. The lowest PdI (0.270 ± 0.00688 and 0.270 ± 0.00622) were obtained with 10% *v*/v of glycerol in physiological solution and 10% v/v of Tween 20 in physiological solution as hydration media, respectively.

It is noteworthy that both ultrasonication and the addition of vesicle bilayer stabilizers produced nanovesicles with low polydispersity. Therefore, a first chemical characterization of the most promising formulations, in terms of recovery of the active compounds, was used as a screening parameter to select the best preparation method. ESN R% (97.5 ± 6.74%) was not affected by ultrasonication. By contrast, CAI-CORM **1** appeared sensitive to this process because R% decreased, probably due to thermal stress. It was 54.0 ± 2.49% for escinosomes sonicated 10 min at 3 cycles (escinosomes with the lowest PdI among those obtained by ultrasonication), and we visually observed a change in the color of the formulation from red to grey and a slight fume emission. The highest recoveries were found for escinosomes stabilized by adding glycerol and Tween 20, besides for no optimized escinosomes (Table 5). Thus, the EE% of CAI-CORM **1** was calculated for the two formulations obtained by adding polyols or surfactants as a second step to assess the adequate hydration medium. ESN EE% was high for both formulations (Table 5); conversely, CAI-CORM **1** EE% was 70.4 ± 2.72% for escinosomes prepared with 10% *v*/v glycerol in physiological solution and 90.1 ± 5.91% for escinosomes prepared with 10% v/v Tween 20 in physiological solution (Table 5). Therefore, the mixture with 10% v/v Tween 20 was chosen as the lipid film hydration solution.

The addition of the surfactant resulted in the best approach to reduce the polydispersity and obtain homogeneous samples easily. In the final formulation, ESN R% was 98.4 ± 2.27%, and ESN EE% was 91.6 ± 8.46% (Table 5). In addition, as the formulation demonstrated a decrease of PdI (0.220 ± 0.0186) after one night of storage at 4 °C, it was let to stabilize in the fridge before any further *in vitro* or *in vivo* study. The ζ-potential was also measured, resulting in −17.3 ± 0.824 mV.

Table 2
Data obtained after extrusion of CAI-CORM **1**-loaded escinosomes. Results are displayed as mean ± SD ($n = 3$).

Membrane pores (nm)	Number of passages	Size (nm)	PdI
/	0	448 ± 7.55	0.429 ± 0.0150
400	11	186 ± 0.857	0.323 ± 0.00590
400	21	189 ± 3.37	0.373 ± 0.0328
400	31	182 ± 0.869	0.394 ± 0.00436
400	51	203 ± 1.04	0.385 ± 0.00780
200	11	190 ± 2.48	0.343 ± 0.0225
200	21	182 ± 1.72	0.364 ± 0.0183
200	31	185 ± 1.67	0.362 ± 0.0247
200	51	187 ± 0.601	0.381 ± 0.00437
400 + 200	31 + 11	222 ± 0.953	0.381 ± 0.00643
400 + 200	31 + 21	229 ± 1.80	0.342 ± 0.0287
400 + 200	31 + 31	220 ± 4.36	0.331 ± 0.0214
400 + 200	31 + 51	219 ± 2.06	0.337 ± 0.0260

/ = no extrusion.

Table 3
Data obtained by ultrasonication of CAI-CORM **1**-loaded escinosomes. Results are displayed as mean ± SD ($n = 3$).

Sonication cycles (second/10)	Sonication time (minutes)	Size (nm)	PdI
1	5	202 ± 1.49	0.385 ± 0.0165
1	10	204 ± 0.982	0.322 ± 0.0268
2	5	163 ± 0.120	0.302 ± 0.0127
2	10	135 ± 2.15	0.332 ± 0.0332
3	5	109 ± 0.285	0.292 ± 0.00674
3	10	87.9 ± 1.04	0.260 ± 0.0180

Table 4
Stabilization of CAI-CORM **1**-loaded escinosomes using polyols or surfactants in the hydration medium. Results are displayed as mean ± SD (n = 3).

Hydration medium	Size (nm)	PdI
5% v/v glycerol / PS	188 ± 0.896	0.461 ± 0.0113
10% v/v glycerol / PS	138 ± 7.75	0.270 ± 0.00688
5% v/v propylene glycol / PS	151 ± 0.917	0.390 ± 0.0159
10% v/v propylene glycol / PS	210 ± 2.26	0.398 ± 0.0145
5% v/v tween 20 / PS	170 ± 3.52	0.310 ± 0.0127
10% v/v tween 20 / PS	168 ± 7.92	0.270 ± 0.00622

PS = physiological solution.

Table 5
Chemical characterization of selected CAI-CORM **1**-loaded escinosomes. Results are displayed as mean ± SEM ($n = 3$).

	CAI-CORM 1 R%	CAI-CORM 1 EE%	ESN R%	ESN EE%
No optimization*	98.6±2.94	n.d.	97.5 ±6.74	n.d.
10% v/v glycerol / PS	96.6±0.469	70.4±2.72	98.2 ±3.64	90.5 ±4.85
10% v/v tween 20 / PS	98.7±5.90	90.1±5.91	98.4 ±2.27	91.6 ±8.46

PS = physiological solution; n.d. = not determined; * = reference.

3.3. HPLC-UV-ESI MS analysis of pure and formulated CAI-CORM 1

Developed escinosomes successfully preserved the chemical structure of the loaded active compound CAI-CORM **1**, screening it from the external aqueous medium and allowing it to overcome its very poor solubility in water. The formulation maintained the compound inside the vesicle bilayer with good stability.

To evaluate the stability of CAI-CORM **1** after loading in escinosomes, HPLC-UV-ESI MS analysis was performed on three solutions of CAI-CORM **1**: the pure compound in acetonitrile, the pure compound in escinosomes and the pure compound in water.

In the chromatographic conditions used for the analysis, CAI-CORM **1** showed maximum absorption at 274 nm (± 4 nm), an intense ion at *m/z* 514 corresponding to the ammonium adduct (Fig. 2a), and a retention time of 13.55 (± 0.50) minutes.

Similar signals were obtained from the analysis of the solution of CAI-CORM **1**-loaded escinosomes; in the UV trace, no other chromatographic peaks were observed, while in the ESI-MS trace, less intense signals were present at different retention times, not interfering with the detection of CAI-CORM **1** (Fig. 2b). These signals were due to the surfactants used in the formulation (as shown in Fig. 2c).

The HPLC-UV-ESI MS analysis of the aqueous solution of CAI-CORM **1** did not show any chromatographic peak due to the compound, probably because of the very poor solubility of this molecule in water. No other signals were detected attributable to the potential degradation of the CAI-CORM **1** molecule either in UV or MS. Therefore, the formulation preparation process did not change the chemical structure of CAI-CORM **1**, and escinosomes loaded it stably.

3.4. Preparation of the thermosensitive gel based on CAI-CORM 1-loaded escinosomes, determination of gelation time and syringeability

Thermosensitive gels incorporating lipid nanovesicles take inspiration from physiological mechanisms. In living cartilage, the embedded chondrocyte cells continuously synthesize lipids and other cartilage components and enable such lipids to accumulate on the surfaces. Hence, lipid nanovesicles within gels can work as a drug and lipid depot, continuously releasing lipids to create lipid-exposing boundary layers, which decrease friction between sliding cartilage tissues [17,18].

Accordingly, we used poloxamer 407 to obtain a thermosensitive gel incorporating CAI-CORM **1**-loaded escinosomes. Poloxamer 407 is an amphiphilic non-ionic surfactant of the triblock-copolymer family of poloxamers. It is recognized as a GRAS (generically recognized as safe) excipient and approved by the U.S. Food and Drug Administration (FDA) for pharmaceutical applications [20]. Poloxamer 407 has been widely studied as a potential biomaterial to obtain thermosensitive hydrogels thanks to its solubilizing capacity, stability in aqueous media, low toxicity and weak immunogenicity, drug release properties, compatibility with numerous biomolecules and excipients, and low viscosity of solutions allowing for ease injection [14,20]. Thermoreversible gels form from concentrated aqueous solutions of poloxamers following increased temperature [14]. Poloxamers are soluble in water at low temperatures due to the formation of stable hydrogen bonds between the central hydrophobic block of poly (propylene oxide) and two hydrophilic terminal blocks of poly (ethylene oxide), and water molecules. At a critical higher temperature, the hydrogen bonds destabilize, and poloxamers self-assemble to form spherical micelles. The micelles' size grows until the poly (propylene oxide) core becomes completely dehydrated, while the outer hydrophilic chains swell and interact to form three-dimensional gel structures [61].

Specifically, the thermosensitive gel of CAI-CORM **1**-loaded escinosomes was prepared by dissolving different percentages of poloxamer 407 in the formulation. Gelation time at 37 °C was evaluated for each mixture by the test tube inverting method (Fig. 3). Percentages lower than 17% gave a gelation time higher than 120 s, whereas the 20% gave a gelation in 80 s, 23% in 40 s, and 25% in 17 s. Therefore, the percentage of 23% was selected since it gave the shortest gelation time and, at the same time, optimal syringeability and injectability, namely the feasibility of withdrawing and releasing the formulation with a 26-gauge syringe needle, which was used for the *in vivo* administration. The ease of syringeability was assessed qualitatively [32,62]. According to our findings, solutions of poloxamer 407 at concentrations of 15–30% *w*/w have a low critical solution temperature like that of normal body temperature, so they can easily be injected by syringe due to the initial low viscosity and control the release of the encapsulated drug by the gelation process [20].

To mimic the injection in the joint cavity and the contact with synovial fluid, we demonstrated the capability of the thermosensitive gel of jellifying at 37 °C also after being injected in water (the test was conducted in water instead of SSF as it requested a large medium volume and without needle to make more visible the sol-gel transition; Videos 1 and 2 of Supplementary Material). The presence of water did not affect the gelation properties of the formulation, which passed to the semisolid state after 40 s, as observed by the test tube inverting method. This simulation highlighted the formulation's ability to remain *in situ* after the administration, thanks to the acquired higher viscosity [32,62]. As the administration requested about half a minute, no immediate gelation was preferable during these studies to prevent needle warming from hindering the formulation release and instantaneous gelation of the first administered amount in the injection site from inducing a greater resistance in releasing the rest of the formulation. By contrast, it is reported that a slight delay between the injection and phase transition into the semisolid gel (Koland et al. reported gelation times longer than 30 s [14]) induces formulation diffusion, interfering with the intended control drug release and viscosupplementation effect [14]. However, considering the injection and gelation time of the developed formulation, we expect a negligible diffusion in the joint cavity after administration. This is also supported by Video 1 of Supplementary Material which shows a certain retention of the liquid formulation in water on the bottle's bottom.

Notably, some authors recently reported on a temperature-sensitive hydrogel based on nanoparticles formulated for the intra-articular administration route, with a sol-gel transition time of about 38 s at (36 ± 1)°C [63]. However, to the best of our knowledge, the formulation we developed represents the first thermosensitive gel based on nanovesicles, specifically escinosomes, for the intra-articular injection, which jellifies in such a short time (40 s) at 37 °C.

R% and EE% of CAI-CORM **1** and ESN were calculated for the obtained thermosensitive gel. No variation due to the addition of poloxamer 407 was observed. CAI-CORM **1** R% was 98.9 ± 5.26%, and ESN R % was 96.0 ± 0.817%, while CAI-CORM **1** EE% was 98.6 ± 1.98%, and ESN EE% was 92.4 ± 9.34%.

3.5. Morphological analysis and thermosensitive gel stability in simulated synovial fluid

CAI-CORM **1**-loaded escinosomes and the corresponding thermosensitive gel were analyzed by electron microscopy to observe the nanovesicles' morphology, dimension, and distribution. The micrograph

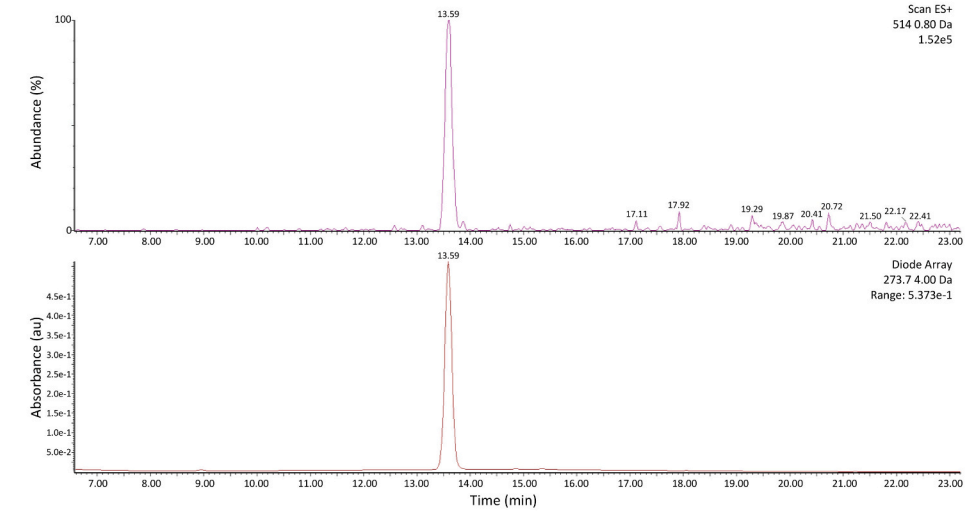

(a)

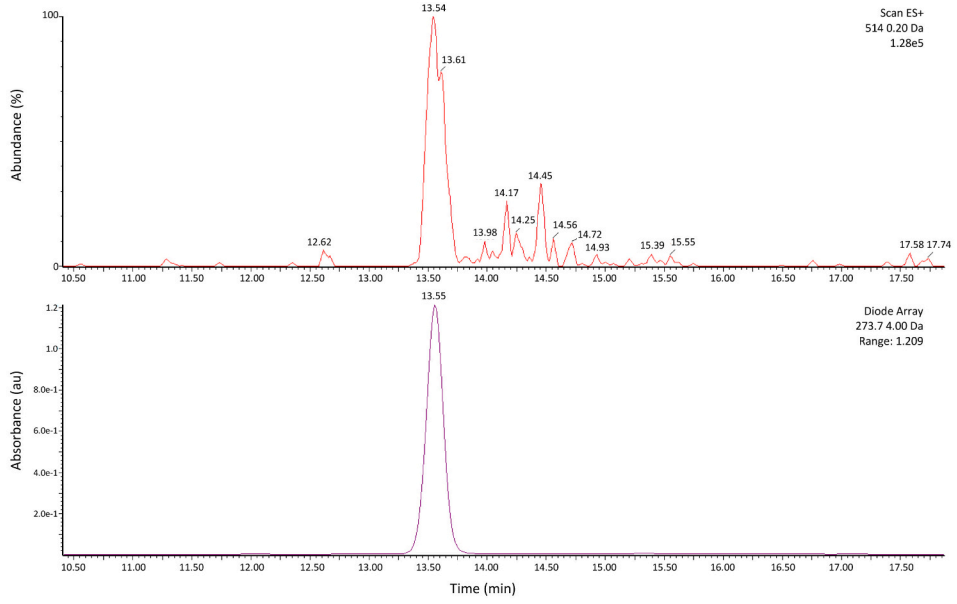

(b)

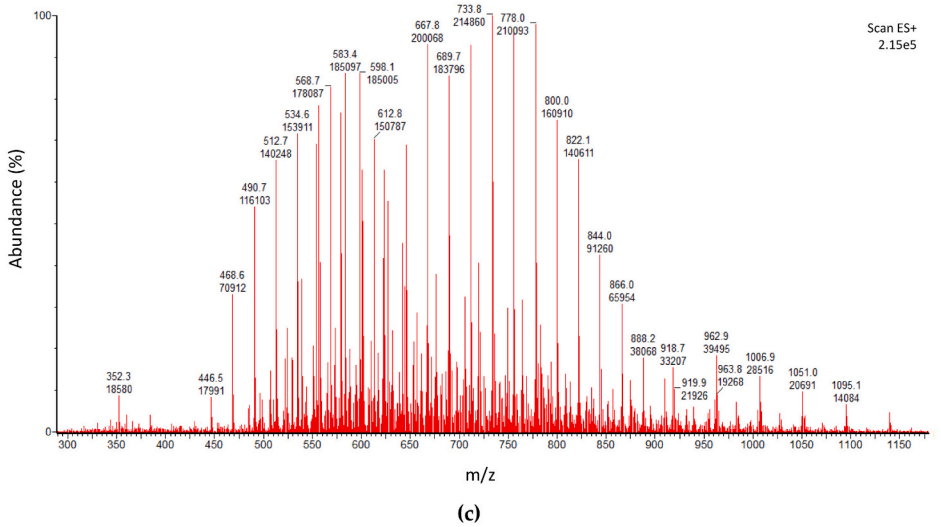

(c)

Fig. 2. CAI-CORM **1** analysis by HPLC-UV-ESI MS. Extracted ion chromatogram of *m/z* 514 (top) and chromatographic profile at 273.7 nm (down) recorded from the analysis of the acetonitrile solution of pure CAI-CORM **1 (a);** extracted ion chromatogram of *m/z* 514 (top) and chromatographic profile at 273.7 nm (down) recorded from the analysis of the solution of CAI-CORM **1**-loaded escinosomes **(b)**; ESI mass spectrum recorded at 14.33 min from the analysis of the solution of CAI-CORM **1**-loaded escinosomes **(c)**.

(a) **(b)**

Fig. 3. Sol-gel transition. Sol form at 25 °C **(a)** and gel form at 37 °C **(b)**.

acquired by TEM (Fig. 4) shows many small and spherical vesicles and a magnification where the lamellarity of some vesicles is visible. In addition, the escinosomes remained stable after adding poloxamer 407 (data not shown).

The thermosensitive gel stability in SSF was evaluated as a predictive study by morphological analysis at time zero, after mixing the thermosensitive gel with SSF, and after 14 days at the end of the incubation time. The stability study was conducted for 14 days at 37 °C to simulate the *in vivo* test conditions. Fig. 5a shows two micrographs obtained by STEM of thermosensitive gel diluted 1:1 in SSF. Vesicles are stable in the synovial liquid, maintaining the shape and dimensions observed for the thermosensitive gel. Fig. 5b displays vesicles after 14 days of incubation with SSF. No evident morphological change is appreciable. The thermosensitive gel stability in contact with SSF for two weeks can be predictive of the good physical stability of the vesicles during the *in vivo* studies.

3.6. Viscosity test

Viscosity is a critical rheological parameter affecting the formulation's application and *in vivo* performance. In the case of a thermosensitive gel for intra-articular administration, if the viscosity is too high, it will make the gel difficult to apply, but if the viscosity is too low, it will make the gel unable to jellify and subjected to the joint clearance [64].

Therefore, the viscosity of the developed thermosensitive gel based on CAI-CORM **1**-loaded escinosomes was evaluated at (25 ± 1)°C (injection temperature) and (37 ± 1)°C (body temperature) by the rotational viscometer. All viscosity measurements were plotted on a graph (Fig. 6), which displays viscosity's up and down rate curves as a function of the spindle rotational speed. At 25 °C, the thermosensitive gel showed a constant viscosity (average value of 441 ± 6.35 mPa×s) at different rotational speeds (30, 50, 100 rpm) using a 03 spindle (Fig. 6). At lower speeds, the viscosity measurement did not provide on-scale readings (torque percentage between 10 and 100), namely, no reliable values. On the other hand, 100 rpm was the highest measurable speed. According to these findings, the thermosensitive gel behaves as a Newtonian fluid at 25 °C. Viscosity is an important fluid property directly affecting both the syringeability and the injectability. Viscosity allows us to predict formulation performance in real-world applications and ensure that formulation can be readily withdrawn and delivered without an excessive injection force, impacting both efficacy and patient compliance [65]. The viscosity values and Newtonian properties observed for the thermosensitive gel at 25 °C were consistent with those obtained by other authors [66–68]. Furthermore, in practice, the obtained viscosity was not shown to negatively affect the injectability, which required about 30 s using a 26-gauge syringe needle.

By contrast, at 37 °C, the gel had different viscosities at different rotational speeds (1, 5, 10, 30, 50, 100 rpm) using a 07 spindle (Fig. 6), able to provide on-scale readings throughout the speed range. Viscosity, for compared rotational speeds (100, 50, 30 rpm), ranges from $5.13\times10^4 \pm 7.36\times10^3$ mPa×s at 30 rpm to $1.47\times10^4 \pm 2.30\times10^3$ mPa×s at 100 rpm. Moreover, Fig. 6 shows that up and down viscosity ramps perfectly overlap. It means that the viscosity does not change as a function of time at a specific rotational speed. Therefore, the thermosensitive gel behaves as a non-Newtonian and time-independent fluid at 37 °C. Specifically, as the viscosity decreases with the increase in rotational speed, the thermogel also performs, similarly to the synovial fluid, as a pseudoplastic and shear thinning fluid [62]. Some authors observed that the shear viscosity of the synovial fluid in osteoarthritis or rheumatoid arthritis-affected joints varied from 0.05 to 14.05 Pa×s, whereas, in healthy joints, the zero shear viscosity was in the range of 1–175 Pa×s [69]. Therefore, it was proposed that the *in situ* gelation upon intra-articular injection would increase the viscosity of the synovial fluid, which could act as a cushioning material to relieve joint pain and discomfort [70]. On the other hand, the achieved high viscosity at 37 °C, also reported by other authors [64,67,71], can predict good retention of the thermosensitive gel after being injected into the joint [62].

Notably, the thermosensitive gel viscosity hugely increased with the temperature change from 25 °C to 37 °C. Specifically, the gel viscosity at 37 °C results from about 30- to 100-fold higher than that measured at 25 °C. These findings were consistent with the literature data since it is reported that gelation induces an approximately 50-fold increase in viscosity when passing from 8 to 37 °C [14]. The change in viscosity is attributable to the thermosensitivity of poloxamer 407. In fact, poloxamer 407-based gels show a liquid-like behavior at low temperatures (*i.e.*, room temperature) and a solid-like behavior at higher temperatures (*i.e.*, body temperature), depending on the poloxamer concentration

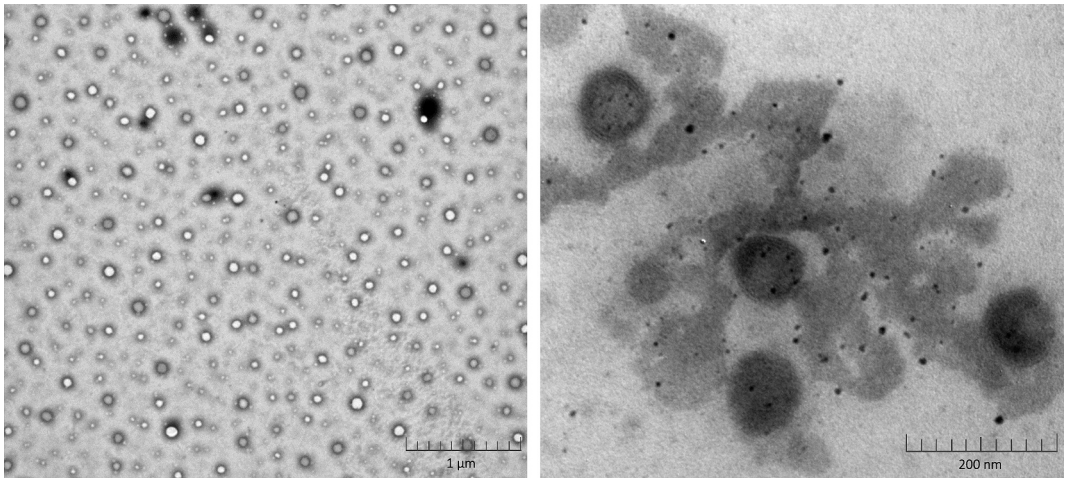

Fig. 4. Morphological characterization by transmission electron microscopy. Pictures of: CAI-CORM 1-loaded escinosomes.

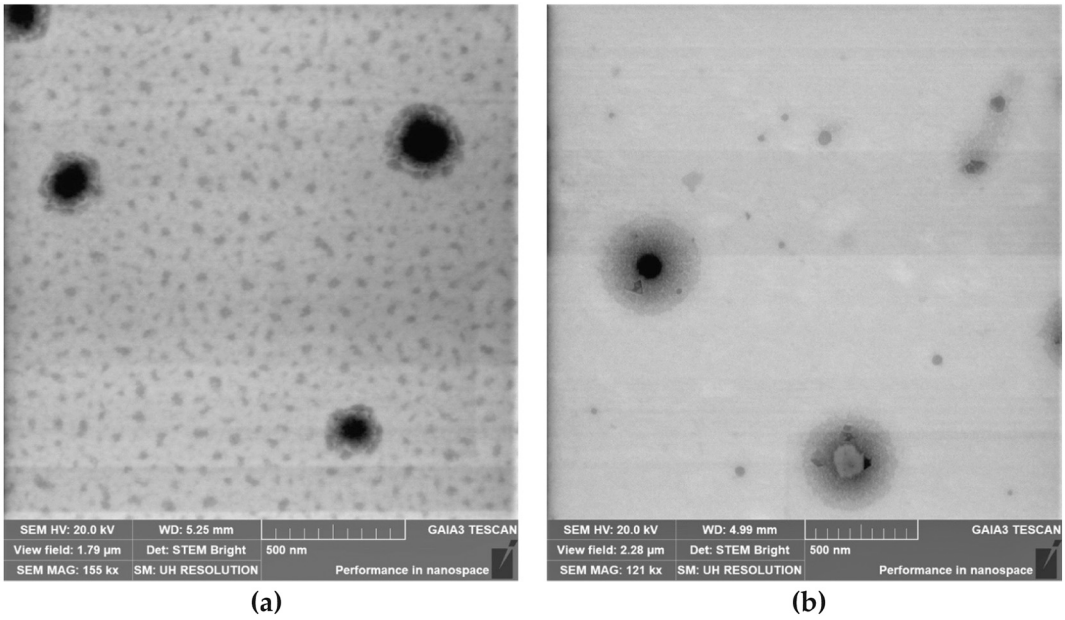

Fig. 5. Stability of the thermosensitive gel of CAI-CORM **1**-loaded escinosomes in simulated synovial fluid. Pictures were obtained by scanning and transmission electron microscopy at time zero **(a)** and after 2 weeks of incubation **(b)**. Scale bar = 500 nm.

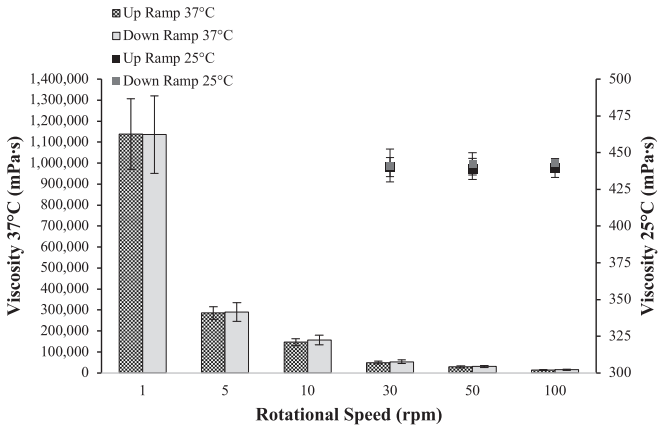

Fig. 6. Viscosity of the thermosensitive gel of CAI-CORM 1-loaded escinosomes measured at (37±1)°C and (25±1)°C. Up and down viscosity ramps (curves obtained from the spindle rotational speed increasing and decreasing, respectively). Data are shown as mean ± SD (n = 3).

[72]. The degree of crosslinking of the poloxamer molecular chain is affected by temperature: high temperatures lead to high degrees of crosslinking. Therefore, poloxamer 407-based gels gradually change from low-viscosity sols to high-viscosity gels when the temperature increases [64,68]. This thermosensitivity permits an easy intra-articular administration (liquid state) and a contemporary viscosupplementation and retention in the joint cavity allowing for a sustained drug release (gel state) [72].

3.7. Drug release study from the thermosensitive gel based on CAI-CORM 1-loaded escinosomes

Gel erosion and passive diffusion are the mechanisms that control the drug release from poloxamer-based *in situ* gelling thermoresponsive systems incorporating nanovesicles [14,61,73]. The rate-limiting step for release varies according to many factors, such as the composition of the gel matrix, the embedded nanocarrier type, the physicochemical properties of the loaded drug, and the environmental conditions of release [14,61,73]. The related tests were carried out to estimate the *in vivo* release properties of the developed formulation.

3.7.1. Thermosensitive gel erosion

The micellar packing arrangement of poloxamers rapidly dissociates in the presence of a high volume of aqueous media leading to the erosion of the gel matrix and, consequently, the release of incorporated nanovesicles. Gel erosion is the primary release mechanism when the loaded drug molecule has a high molecular weight [14,61,73]. Similarly, we can expect embedded nanovesicles to release following gel erosion due to the low mobility of the large structures through the internal aqueous channels to the external environment.

The erosion of the thermoreversible gel incorporating CAI-CORM **1**-loaded escinosomes was investigated by the gravimetric method using the membrane-less model [41–43], according to the potential clinical use of the gel *via* intra-articular injection. The formulation was placed in an Eppendorf tube and warmed in a water bath at 37 °C until gel formed (Fig. 7a, Experiment Setup). The SSF was also pre-equilibrated at 37 °C and layered over the gel surface (Fig. 7a, Experiment Setup). Fig. 7b shows how the gel dissolution appears during the experiment. The cumulative erosion rate curve was constructed by plotting the cumulative erosion rate on the y-axis and time on the x-axis (Fig. 7b). It achieved the 88.2 ± 0.743% within 9 h. After 10 h, separating the gel from the SSF distinctly was not feasible. These findings were consistent with previous research [42]. When the gel dissolves in the synovial fluid of the joint cavity, it releases CAI-CORM **1**-loaded escinosomes. Free drug diffusion out of the gel matrix can be considered negligible during the erosion process, as the EE% inside escinosomes was high for both ESN and CAI-CORM **1**. Also, the micelle's compact arrangement, especially in gels with a greater degree of crosslinking due to the higher poloxamer concentration, decreases the number and size of aqueous channels and, consequently, slows drug diffusion [14,61]. Similarly, we expected the swollen gel matrix and increased viscosity to slow the drug diffusion across the nanovesicle bilayer. Therefore, assuming the drug release from escinosomes starts as soon as loaded nanovesicles are released in the synovial fluid, we mixed the thermosensitive gel with SSF in a liquid state mimicking the conditions of the gel dissolved in the joint cavity, and we performed the passive diffusion test to predict the release rate *in vivo*.

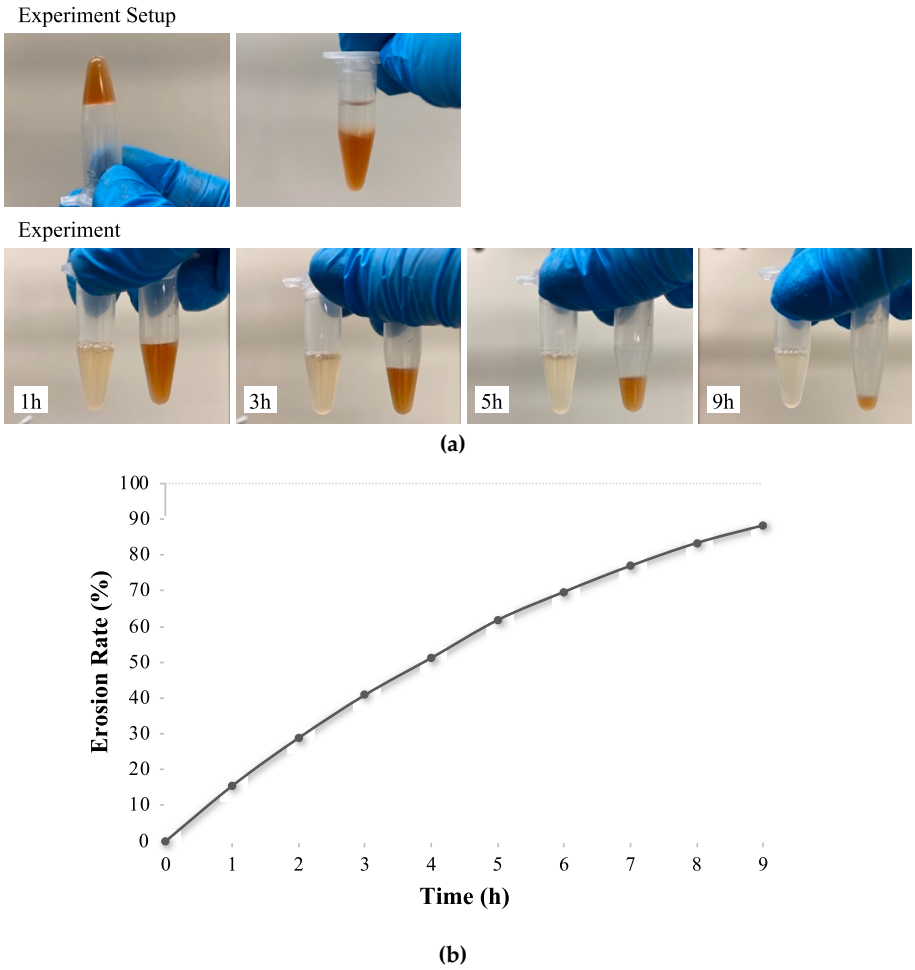

Fig. 7. Experiment setup and illustration of the erosion process of the thermosensitive gel incorporating CAI-CORM 1-loaded escinosomes in simulated synovial fluid at 37 °C **(a).** Erosion rate curve as a function of time **(b)**. Data are shown as mean ± SD ($n = 3$).

3.7.2. *Passive diffusion of CAI-CORM-1 from escinosomes*

Loading the drug in nanovesicles embedded in the thermoreversible gel helps to avoid a burst effect due to the gel erosion and passive diffusion through the aqueous channels of the gel matrix, providing a further *in situ* depot and a sustained release into the surrounding tissues after gel dissolution. Therefore, the release rate of ESN and CAI-CORM **1**

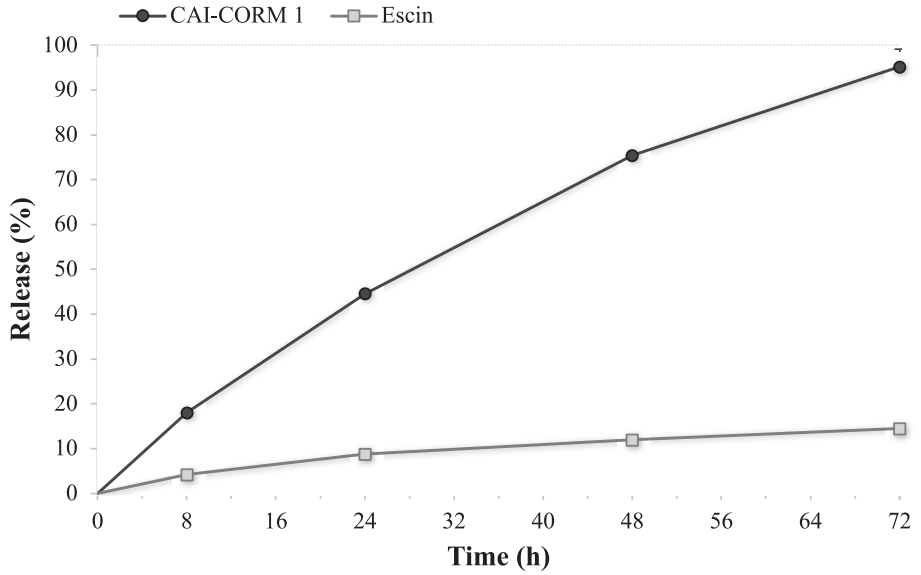

Fig. 8. The release rate of CAI-CORM **1** and escin from escinosomes. Data are shown as mean ± SD ($n = 3$).

from escinosomes was investigated by the dialysis bag method. The thermosensitive gel was mixed with SSF in a liquid mixture, reproducing the conditions after gel dissolution in the synovial fluid. The release of the active compounds was monitored for 72 h, and data were plotted on a graph (Fig. 8). ESN release was found to be minimal, reaching 14.47 ± 3.031% over 72 h. This result demonstrates the physical stability of escinosomes, as evidenced in previous studies [21,22], as the small ESN release can be attributed to only a partial nanocarrier degradation over time, confirming their drug depot function.

By contrast, we could not track CAI-CORM **1** in the acceptor medium during the experiment, and we analyzed the bag content, expressed as R %, to determine the percentage of the released drug by an indirect method. CAI-CORM **1**, still loaded inside escinosomes in the bag, was effortlessly detected. The graph in Fig. 8 shows a prolonged release of CAI-CORM **1**, achieving 95.15 ± 0.01004% within 72 h. Moreover, similar results were obtained performing the same test with the thermogel diluted in a 1:1 volumetric ratio in PBS, excluding a possible interference due to SSF components (data not shown). The formulation mixed with SSF or PBS and stored for the same period of the release tests did not show a comparable decrease in CAI-CORM **1** concentration, confirming the involvement of the release process in determining the observed reduction in CAI-CORM **1** R%.

These findings highlighted the critical role of the formulation in the stability of the loaded active molecule. Escinosomes showed to protect CAI-CORM **1** from the external environment of the joint cavity until it is released, providing an efficacious *in situ* depot.

The carried out study confirmed that the mechanisms of gel erosion and passive drug diffusion interweave in contributing to the drug release process. Incorporating CAI-CORM **1**-loaded escinosomes into a poloxamer-based *in situ* gel increases drug residence time and sustains drug release by creating multiple rate-limiting release barriers [13,61]. Notably, the slow gel erosion over 10 h and slow passive diffusion across the escinosome bilayers over 72 h allow a prolonged and sustained release of CAI-CORM **1**, which in turn expectably degrades to release CO, as in agreement with the reported literature [11]. It is well known that CORMs tend to dissociate according to different mechanisms not yet defined and dependent on solvent and microenvironment [11]. Cobalt-based CORMs are reported to be stable in PBS for up to 6 h, but the low aqueous solubility makes their detection quite tricky at the used concentration [74]. The effective CO release from the CORM occurring when the molecule is released within the SSF (or the inflamed joint *in vivo*) is much more complex and difficult to predict and monitor at this stage. Escinosomes provide a further *in situ* depot protecting the active molecule from immediate degradation after gel erosion.

Rheumatoid arthritis is a chronic disease, and frequent administration is needed, but it can lead to nerve damage, synovial membrane inflammation, or bacterial infections [13,70]. The sustained-release preparations for intra-articular injection can improve patients' compliance with a few injections and, consequently, treatment efficacy [13]. Several hyaluronic acid hydrogels are currently available as a viscosupplementation technique on the market [70]. Also, a triamcinolone acetonide extended-release formulation (Zilretta®) was approved in the USA for managing knee osteoarthritis pain and is administered as a single intra-articular injection [75]. The formulation developed in our study fits brilliantly into this scenario, proposing a practical pharmacological approach combined with an innovative dosage form.

3.8. *In vivo experiments*

Rheumatoid arthritis is mainly an inflammatory-erosive joint disease affecting 2% of the population worldwide, causing severe debilitating morbidity and high economic cost because of the progressive joint destruction, swelling, deformity, and pain that ultimately hamper basic mobility functions, significantly reducing the patient's quality of life [76,77]. Traditional treatments like anti-inflammatory drugs effectively reduce inflammation and pain [5,78] but, used routinely, cause several side effects, including gastrointestinal irritation, interstitial lung disease, and osteoporosis [79]. For instance, finding novel therapeutic approaches for effective treatments and avoiding side effects is urgent. Intra-articular therapy is a cornerstone procedure extensively used for treating patients with joint synovitis, effusion, and pain of different origins, such as osteoarthritis and rheumatoid arthritis. Corticosteroids are the most recommended therapies for managing articular pain [68,69] despite not being free from adverse reactions and complications [80,81]. Thus, their overall risk ratio is considered unfavorable [82]. In this study, we assessed, by the intra-articular route, the anti-hypersensitivity effect of a single injection of CAI-CORM **1** formulation (thermosensitive gel of CAI-CORM **1**-loaded escinosomes) in a rat model of rheumatoid arthritis induced by CFA injection. The efficacy of this formulation was compared with the activity of the blank formulation (thermosensitive gel of unloaded escinosomes). CFA intra-articular injection is an established and well-characterized animal model of rheumatoid arthritis that determines the release of pro-inflammatory cytokines from inflammatory cells leading to cartilage erosion and bone destruction [23,83]. Previous studies had demonstrated that CFA injection evoked spontaneous pain, decreasing the weight the animals bear on the ipsilateral paw compared to the contralateral one, hyperalgesia and allodynia when acute applications of noxious and non-noxious stimuli were applied, respectively, and motor impairments [49]. The painful condition started 3 days after CFA injection, peaking after 2 weeks [49]. In this study, the two formulations were intra-articular injected only once when the painful condition was already established (7 days after the damage with CFA). Their efficacy was assessed 7 and 14 days after treatment. CFA significantly reduced the pain threshold of the ipsilateral paws on both analyzed days (7 and 14) compared to the control group treated with vehicle (vehicle + vehicle; Fig. 9). The single intra-articular injection of CAI-CORM **1** significantly improved the weight tolerated on the ipsilateral paws, increasing the efficacy over time, while the treatment with the blank formulation was ineffective (Fig. 9). The pain-relieving properties of the CAI-CORM **1** hybrid molecule were previously highlighted in the same animal model of articular pain following a systemic administration [11]. We moved to

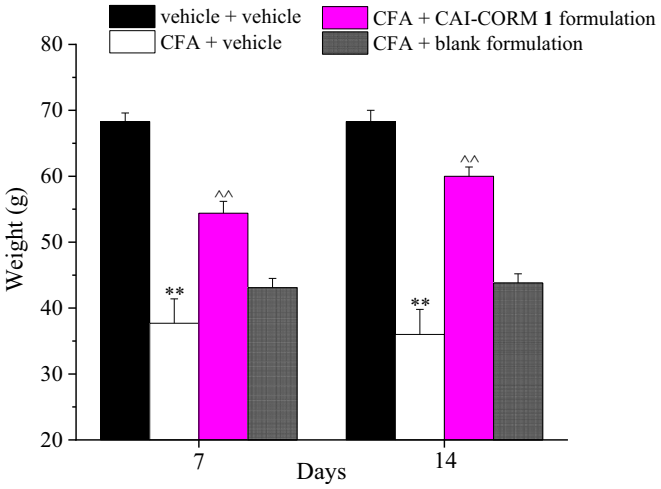

Fig. 9. Articular pain related to mechanical hyperalgesia. Rheumatoid arthritis was induced by CFA injection (50 μL) into the tibio-tarsal joint (day −7). Thirty μL of CAI-CORM **1** formulation (3 mg/mL) or blank formulation were intra-articular administered 7 days after CFA injection (day 0). The Paw pressure test was performed on days 7 and 14 after treatments with the formulations to assess the hypersensitivity toward a noxious mechanical stimulus. (CAI-CORM **1** formulation = thermosensitive gel of CAI-CORM **1**-loaded escinosomes; blank formulation = thermosensitive gel of unloaded escinosomes). Each value represents the mean ± SEM of six rats per group performed in two different experimental sets. $^{**}P<0.01$ *vs* vehicle + vehicle group; ^^P<0.01 *vs* CFA + vehicle group.

a single local administration of the compound to avoid systemic exposure caused by the repeated treatment usually required for the management of chronic pain. To this purpose, CAI-CORM **1** was loaded in escinosomes embedded in a thermosensitive hydrogel, allowing a prolonged drug release by forming a depot in the joint cavity, thus avoiding repeated administrations. Moreover, ESN, a bioactive constituent of *Aesculus hippocastanum*, is endowed with a beneficial role because of its anti-inflammatory, anti-edematous, and anti-oxidative effects [53]. Accordingly, previous studies demonstrated that ESN combined with low doses of corticosteroids improved their anti-arthritic effect [52,53].

The single intra-articular treatment with CAI-CORM evoked similar results also when a non-noxious mechanical stimulus was applied to the animals (von Frey test; Fig. 10). Only the CAI-CORM **1** formulation significantly increased the ipsilateral paws' withdrawal threshold compared to CFA + vehicle-treated rats. As reported in the previous test, the hybrid molecule's efficacy slightly increased over time. This is an important issue that highlights the formulation's long-lasting effect due to the formation of a gel depot. The injection of the thermosensitive gel of unloaded escinosomes (CFA + blank formulation) was inactive, underling that viscosupplementation and lubrification, associated with the nanovesicle phospholipids and the hydrogel [14,17,18], are not enough to counteract the progression of arthritis despite the previously described properties of escin.

Monolateral pain induced by CFA was also able to evoke spontaneous pain, measured by the Incapacitance test and reported as Δ weight between the weight burdened by rats on the contralateral minus the ipsilateral paw (Fig. 11). In this test, no nociceptive or non-nociceptive stimuli were applied to rats to analyze the treatment's efficacy against spontaneous pain. The Δ weight is more than quadrupled in CFA-treated animals compared to the control group, and the CAI-CORM **1** formulation treatment has rebalanced this gap on both days, while the blank formulation was unable to restore postural unbalance (Fig. 11). The blank formulation was ineffective even in this case, although the results obtained in this group were lower than those of the untreated animals with articular pain (CFA + vehicle).

Lastly, motor impairments were also evaluated by the beam balance test. CFA injection significantly increased motor incoordination and staggering walking, as reported in Fig. 12. The pathological score in CFA + CAI-CORM **1** formulation-treated animals was reduced both on day 7 and on day 14, indicating a partial recovery from the damage even if the values of control animals were not reached. The blank formulation was inactive.

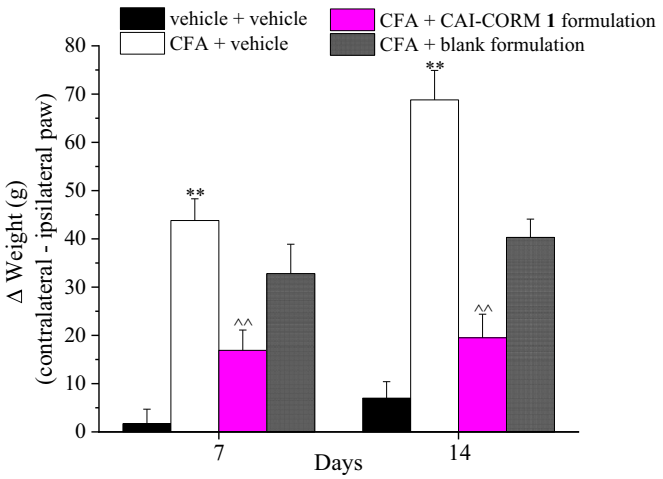

Fig. 11. Articular spontaneous pain. Rheumatoid arthritis was induced by CFA injection (50 μL) into the tibio-tarsal joint (day −7). Thirty μL of CAI-CORM **1** formulation (3 mg/mL) or blank formulation were intra-articular administered 7 days after CFA injection (day 0). The Incapacitance test was performed on days 7 and 14 after treatments with the formulations to assess their effect on spontaneous pain. (CAI-CORM **1** formulation = thermosensitive gel of CAI-CORM **1**-loaded escinosomes; blank formulation = thermosensitive gel of unloaded escinosomes). Each value represents the mean ± SEM of six rats per group performed in two different experimental sets. ***P*<0.01 *vs* vehicle + vehicle group; ^^P<0.01 *vs* CFA + vehicle group.

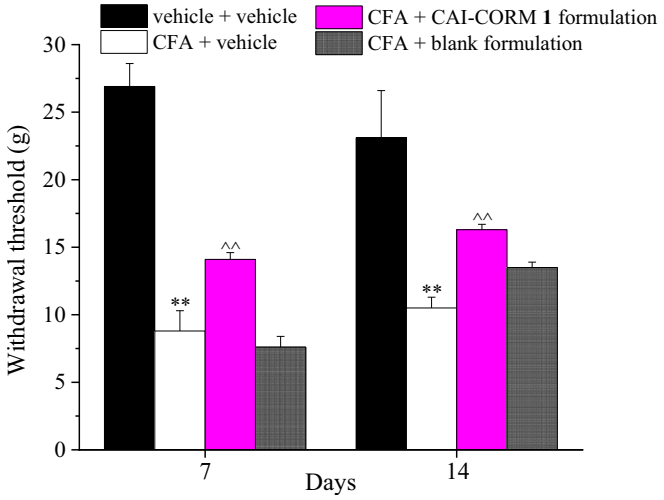

Fig. 10. Articular pain related to mechanical allodynia. Rheumatoid arthritis was induced by CFA injection (50 μL) into the tibio-tarsal joint (day −7). Thirty μL of CAI-CORM **1** formulation (3 mg/mL) or blank formulation were intra-articular administered 7 days after CFA injection (day 0). The von Frey test was performed on days 7 and 14 after treatments with the formulations to assess the hypersensitivity toward a non-noxious mechanical stimulus. (CAI-CORM **1** formulation = thermosensitive gel of CAI-CORM **1**-loaded escinosomes; blank formulation = thermosensitive gel of unloaded escinosomes). Each value represents the mean ± SEM of six rats per group performed in two different experimental sets. ***P*<0.01 *vs* vehicle + vehicle group; ^^P<0.01 *vs* CFA + vehicle group.

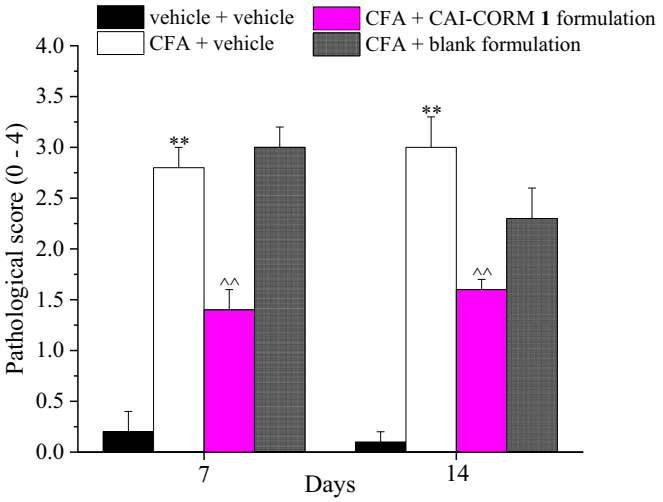

Fig. 12. Motor abilities related to pain. Rheumatoid arthritis was induced by CFA injection (50 μL) into the tibio-tarsal joint (day −7). Thirty μL of CAI-CORM **1** formulation (3 mg/mL) or blank formulation were intra-articular administered 7 days after CFA injection (day 0). The beam balance test was performed on days 7 and 14 after treatments with the formulations to assess their effect on motor alterations. (CAI-CORM **1** formulation = thermosensitive gel of CAI-CORM **1**-loaded escinosomes; blank formulation = thermosensitive gel of unloaded escinosomes). Each value represents the mean ± SEM of six rats per group performed in two different experimental sets. ***P*<0.01 *vs* vehicle + vehicle group; ^^P<0.01 *vs* CFA + vehicle group.

3.9. Ex vivo analysis

At the end of the behavioral studies, the animals were sacrificed, and histological analysis of the tibio-tarsal joint was performed. The damage with CFA determined an increase in inflammation, synovial hyperplasia, and vascularity, cartilage, and bone erosion, as well as fibrin deposition and a reduction of the joint space. The single intra-articular treatment with CAI-CORM **1** formulation significantly rebalanced all parameters evaluated, except for bone erosion (Fig. 13). The blank formulation containing only escinosomes was found to be active in reducing the inflammatory infiltrate, synovial hyperplasia, fibrin deposition, and cartilage erosion, indicating a positive effect also from the empty escinosomes. This function was attributed to the formation of a gel deposit which can impart viscosupplementant and lubricant actions. Moreover, a certain activity could be due to escin, widely studied for its anti-inflammatory properties in reducing vascular permeability in inflamed tissues, thereby inhibiting edema formation [84].

4. Conclusions

Rheumatoid arthritis is a debilitating disease that causes chronic pain, negatively affecting the patient's quality of life. Although several drugs are available, such as NSAIDs and corticosteroids, current therapeutic strategies have limited efficacy, high costs, or low patient compliance. Also, the traditional dosage forms are inefficient in the long-term treatment of chronic inflammatory disorders of joints [1–4]. Recent FDA approvals of various intra-articular gels demonstrate the market interest in sustained-release formulations for intra-articular therapy [14]. All these reasons lead to the necessity of new pharmacological and formulation approaches to improve the clinical management of rheumatoid arthritis. Thermoreversible gels incorporating lipid nanovesicles can be considered valuable dosage forms for this purpose. The gelation at body temperature after intra-articular injection can minimize rapid drug clearance from the joint cavity and prolong its release. Lipid nanovesicles can protect the active ingredient from the joint environment until it is released and contribute to retaining drugs in the joint, reducing the dosing frequency. Both systems provide lubricating and viscosupplementation properties [13,19,20]. Temperature-based gelling systems are also reliable as their properties do not vary much between individuals [14].

In this study, we developed a thermosensitive gel incorporating escinosomes to formulate CAI-CORM **1** in a suitable dosage form for intra-articular injection. The formulation was designed to overcome its low solubility in water and prolong its chemical stability in the synovial fluid. *In situ* gelification has been considered a key feature in achieving a prolonged drug release and partially restoring the physiological intra-articular viscosity temporarily. The aim of the study was successfully attained by optimizing a safe delivery system and the drug's efficacy by a single intra-articular administration in a rat model of rheumatoid arthritis.

Carbonic anhydrase inhibitors (CAIs) have many potential clinical applications, and they can be hybridized with various other diverse pharmacological agents, acting on additional targets to achieve better therapeutic outcomes [85]. Recently, CAI–CO releasing molecular hybrids (CAI-CORM) have been synthesized, considering the well-documented activity of CO as a gas-transmitter, mediating important cytoprotective effects and being involved in various biological processes, including inflammation, microbial infections, CNS signaling, and apoptosis [11]. These hybrids have great potential, but their administration by intra-articular route, because of their poor water solubility.

Escinosomes are innovative natural nanovesicles made of phosphatidylcholine and escin, exhibiting high versatility in loading natural and synthetic compounds and preserving drug chemical structure [21,22]. CAI-CORM **1** was effectively loaded in escinosomes, with an EE% of about 99%, using 10% *v*/v of tween 20. Then, escinosomes were formulated in a thermosensitive gel containing 23% *w/v* poloxamer 407, which gelled in 40 s at 37 °C. This percentage gave the shortest gelation time and good syringeability and injectability for *in vivo* administration. The thermosensitive gel's physical stability was evaluated by monitoring the vesicles' morphology in contact with the simulated synovial fluid for two weeks by electron microscopy. CAI-CORM **1** chemical stability in the final formulation was confirmed by HPLC-UV-ESI MS, highlighting the critical role of escinosomes in preserving CAI-CORM **1** stability as observed during the passive diffusion test for the drug release study. Also, the gel erosion, evaluated in the *in vivo* simulating experimental conditions, occurring in 10 h provides a sustained release of drug-loaded escinosomes and slows drug diffusion in the joint environment. The viscosity of the thermosensitive gel increased with the temperature change from 25 °C to 37 °C. This increased *in situ* gel retention and synovial fluid viscosity, consequently relieving joint pain.

This study also demonstrated the anti-hypersensitivity effect of a single intra-articular injection of CAI-CORM **1** loaded in escinosomes and formulated in a thermosensitive gel in a rat model of rheumatoid arthritis induced by CFA injection. Unloaded escinosomes formulated in the thermosensitive gel were inactive, indicating that viscosupplementation and lubrification were insufficient to counteract the arthritis progression. Conversely, the escinosome-based thermosensitive gel reduced inflammatory infiltrate, synovial hyperplasia, fibrin deposition, and cartilage erosion. This function could be attributed to forming a gel deposit, which can impart viscosupplementant and lubricant actions, and to the anti-inflammatory and anti-edematous activities of the saponin.

In conclusion, the developed formulation represents the first attempt at a thermosensitive gel incorporating lipid nanovesicles, specifically escinosomes, successfully investigated for intra-articular administration, stabilization, and sustained release of a lipophilic newly synthesized drug such as the CAI-CORM **1** hybrid. The study highlighted that CAI-CORM **1** formulated in escinosome-based thermosensitive gel exerts optimal anti-rheumatoid activity in the rat model of CFA–induced rheumatoid arthritis with long-lasting efficacy and good tolerability of rats toward escinosomes. Moreover, the promising outcomes reported for the first time in this study pave the way for further investigations on the potential therapeutic application of escinosome-based thermosensitive gel as an intra-articular drug delivery system for managing chronic diseases.

Supplementary data to this article can be found online at https://doi.org/10.1016/j.jconrel.2023.04.045.

Funding

Fabrizio Carta is grateful to "Bando di Ateneo per il Finanziamento di Progetti Competitivi per Ricercatori a Tempo Determinato (RTD) dell'Università di Firenze - 2020-2021," which partially funded this work.

Studies in animals

All animal manipulations were carried out according to Directive 2010/63/EU of the European Parliament and of the European Union council (22 September 2010) on the protection of animals used for scientific purposes. The ethical policy of the University of Florence complies with the Guide for the Care and Use of Laboratory Animals of the US National Institutes of Health (NIH Publication No. 85-23, revised 1996; University of Florence assurance number: A5278-01). Formal approval to conduct the experiments described was obtained from the Italian Ministry of Health (No. 517/2017, 06/04/2017) and the Animal Subjects Review Board of the University of Florence. Experiments involving animals have been reported according to the ARRIVE guidelines [86]. All efforts were made to minimize animal suffering and to reduce the number of animals used.

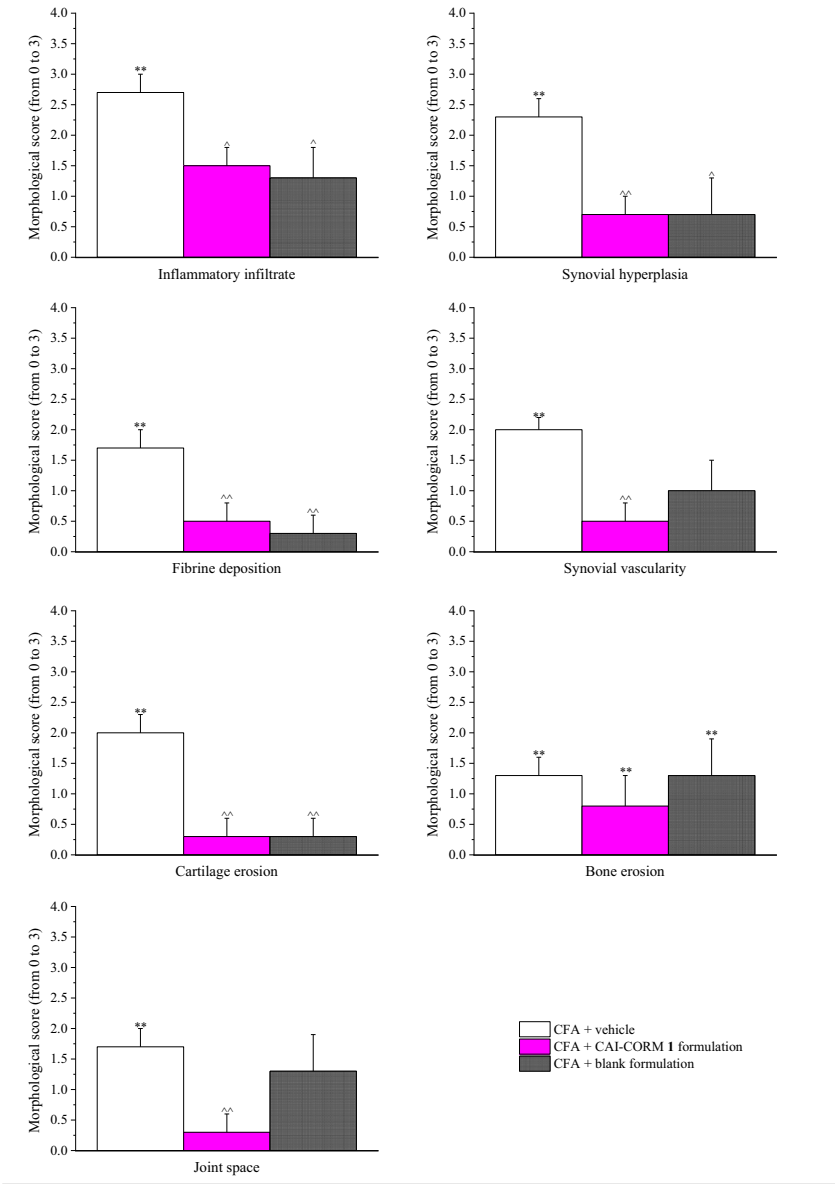

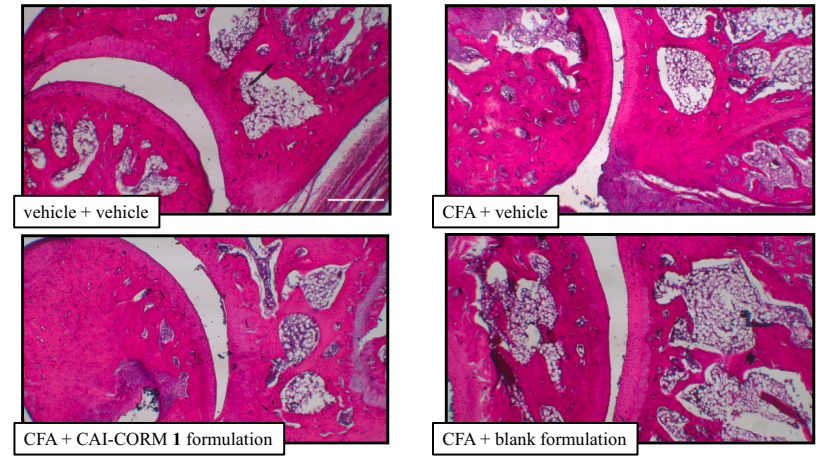

Fig. 13. Morphological evaluations of the tibio-tarsal joints on day 14 after treatments. The panel represents the quantification of the morphological parameters by a specific score (0: absent; 1: light; 2: moderate; 3: severe). The control animals had a morphological score equal to 0 and were not reported in the graphs. (CAI-CORM **1** formulation = thermosensitive gel of CAI-CORM **1**-loaded escinosomes; blank formulation = thermosensitive gel of unloaded escinosomes). Each value represents the mean ± SEM. of six rats per group performed in two different experimental sets. **P<0.01 *vs* vehicle + vehicle group; ^*P*<0.05 and ^^P<0.01 *vs* CFA + vehicle group.

CRediT authorship contribution statement

Giulia Vanti: Conceptualization, Data curation, Formal analysis, Investigation, Methodology, Writing – original draft. **Laura Micheli:** Data curation, Formal analysis, Investigation, Methodology, Validation, Writing – original draft. **Emanuela Berrino:** Data curation, Investigation, Methodology, Writing – original draft. **Lorenzo Di Cesare Mannelli:** Conceptualization, Methodology, Software, Supervision. **Irene Bogani:** Investigation, Methodology. **Fabrizio Carta:** Conceptualization, Funding acquisition, Methodology, Software, Supervision, Writing – review & editing. **Maria Camilla Bergonzi:** Data curation, Methodology, Supervision, Writing – review & editing. **Claudiu T. Supuran:** Funding acquisition, Project administration, Resources, Supervision. **Carla Ghelardini:** Funding acquisition, Project administration, Resources, Supervision. **Anna Rita Bilia:** Conceptualization, Funding acquisition, Project administration, Resources, Supervision, Writing – review & editing.

Declaration of Competing Interest

The authors declare that they have no competing financial interests or personal relationships that could have appeared to influence the work reported in this paper.

Data availability

Data will be made available on request.

Acknowledgments

The authors thank MIUR-Italy ("Progetto dipartimenti di eccellenza 2023-2027" allocated to the Department of Chemistry "Ugo Schiff", University of Florence, Italy). The authors express thanks to the Mass Spectrometry Center (CISM) of the University of Florence for HPLC-UV-ESI MS analyses and Dr. Maria Cristina Salvatici, Electron Microscopy Centre (Ce.M.E.), ICCOM, CNR, Sesto Fiorentino, Florence, Italy for data curation of STEM and TEM.

References

[1] J.E. Lee, I.J. Kim, M.S. Cho, J. Lee, A case of rheumatoid vasculitis involving hepatic artery in early rheumatoid arthritis, J. Korean Med. Sci. 32 (2017), https://doi.org/10.3346/jkms.2017.32.7.1207.

[2] C.K.S. Ong, P. Lirk, C.H. Tan, R.A. Seymour, An evidence-based update on nonsteroidal anti-inflammatory drugs, Clin. Med. Res. 5 (2007), https://doi.org/10.3121/cmr.2007.698.

[3] B. Combe, R. Landewe, C.I. Daien, C. Hua, D. Aletaha, J.M. Álvaro-Gracia, M. Bakkers, N. Brodin, G.R. Burmester, C. Codreanu, R. Conway, M. Dougados, P. Emery, G. Ferraccioli, J. Fonseca, K. Raza, L. Silva-Fernández, J.S. Smolen, D. Skingle, Z. Szekanecz, T.K. Kvien, A. Van Der Helm-Van Mil, R. Van Vollenhoven, Update of the EULAR recommendations for the management of early arthritis, Ann. Rheum. Dis. 76 (2017) (2016), https://doi.org/10.1136/annrheumdis-2016-210602.

[4] D. Liu, A. Ahmet, L. Ward, P. Krishnamoorthy, E.D. Mandelcorn, R. Leigh, J. P. Brown, A. Cohen, H. Kim, A practical guide to the monitoring and management of the complications of systemic corticosteroid therapy, allergy, Asthma Clin. Immunol. 9 (2013), https://doi.org/10.1186/1710-1492-9-30.

[5] J. Bullock, S.A.A. Rizvi, A.M. Saleh, S.S. Ahmed, D.P. Do, R.A. Ansari, J. Ahmed, Rheumatoid arthritis: a brief overview of the treatment, Med. Princ. Pract. 27 (2019), https://doi.org/10.1159/000493390.

[6] R. Agca, S.C. Heslinga, S. Rollefstad, M. Heslinga, I.B. McInnes, M.J.L. Peters, T. K. Kvien, M. Dougados, H. Radner, F. Atzeni, J. Primdahl, A. Södergren, S. Wallberg Jonsson, J. van Rompay, C. Zabalan, T.R. Pedersen, L. Jacobsson, K. de Vlam, M.A. Gonzalez-Gay, A.G. Semb, G.D. Kitas, Y.M. Smulders, Z. Szekanecz, N. Sattar, D.P.M. Symmons, M.T. Nurmohamed, EULAR recommendations for cardiovascular disease risk management in patients with rheumatoid arthritis and other forms of inflammatory joint disorders: 2015/2016 update, Ann. Rheum. Dis. 76 (2016), https://doi.org/10.1136/annrheumdis-2016-209775.

[7] J.A. Roman-Blas, E. Bizzi, R. Largo, A. Migliore, G. Herrero-Beaumont, An update on the up and coming therapies to treat osteoarthritis, a multifaceted disease, Expert. Opin. Pharmacother. 17 (2016), https://doi.org/10.1080/14656566.2016.1201070.

[8] R. Motterlini, L.E. Otterbein, The therapeutic potential of carbon monoxide, Nat. Rev. Drug Discov. 9 (2010), https://doi.org/10.1038/nrd3228.

[9] W. Adach, B. Olas, Carbon monoxide and its donors - their implications for medicine, Future Med. Chem. 11 (2019), https://doi.org/10.4155/fmc-2018-0215.

[10] M.L. Ferrándiz, N. Maicas, I. Garcia-Arnandis, M.C. Terencio, R. Motterlini, I. Devesa, L.A.B. Joosten, W.B. van den Berg, M.J. Alcaraz, Treatment with a CO-releasing molecule (CORM-3) reduces joint inflammation and erosion in murine collagen-induced arthritis, Ann. Rheum. Dis. 67 (2008), https://doi.org/10.1136/ard.2007.082412.

[11] E. Berrino, L. Milazzo, L. Micheli, D. Vullo, A. Angeli, M. Bozdag, A. Nocentini, M. Menicatti, G. Bartolucci, L. di Cesare Mannelli, C. Ghelardini, C.T. Supuran, F. Carta, Synthesis and evaluation of carbonic anhydrase inhibitors with carbon monoxide releasing properties for the management of rheumatoid arthritis, J. Med. Chem. 62 (2019), https://doi.org/10.1021/acs.jmedchem.9b00845.

[12] F. Margheri, M. Ceruso, F. Carta, A. Laurenzana, L. Maggi, S. Lazzeri, G. Simonini, F. Annunziato, M. del Rosso, C.T. Supuran, R. Cimaz, Overexpression of the transmembrane carbonic anhydrase isoforms IX and XII in the inflamed synovium, J. Enzyme Inhib. Med. Chem. 31 (2016), https://doi.org/10.1080/14756366.2016.1217857.

[13] P. Song, Z. Cui, L. Hu, Applications and prospects of intra-articular drug delivery system in arthritis therapeutics, J. Control. Release 352 (2022) 946–960, https://doi.org/10.1016/j.jconrel.2022.11.018.

[14] M. Koland, A. Narayanan Vadakkepushpakath, A. John, A. Tharamelveliyil Rajendran, I. Raghunath, Thermosensitive in situ gels for joint disorders: pharmaceutical considerations in intra-articular delivery, Gels. 8 (2022) 723, https://doi.org/10.3390/gels8110723.

[15] Y. Cao, Y. Ma, Y. Tao, W. Lin, P. Wang, Intra-articular drug delivery for osteoarthritis treatment, Pharmaceutics. 13 (2021), https://doi.org/10.3390/pharmaceutics13122166.

[16] T. Siefen, S. Bjerregaard, C. Borglin, A. Lamprecht, Assessment of joint pharmacokinetics and consequences for the intraarticular delivery of biologics, J. Control. Release 348 (2022) 745–759, https://doi.org/10.1016/j.jconrel.2022.06.015.

[17] W. Lin, J. Klein, Hydration lubrication in biomedical applications: from cartilage to hydrogels, Acc. Mater. Res. 3 (2022), https://doi.org/10.1021/accountsmr.1c00219.

[18] O. Craciunescu, M. Icriverzi, P.E. Florian, A. Roseanu, M. Trif, Mechanisms and pharmaceutical action of lipid nanoformulation of natural bioactive compounds as efficient delivery systems in the therapy of osteoarthritis, Pharmaceutics. 13 (2021), https://doi.org/10.3390/pharmaceutics13081108.

[19] Y. Cao, Y. Ma, Y. Tao, W. Lin, P. Wang, Intra-articular drug delivery for osteoarthritis treatment, Pharmaceutics. 13 (2021), https://doi.org/10.3390/pharmaceutics13122166.

[20] E. Giuliano, D. Paolino, M. Fresta, D. Cosco, Drug-loaded biocompatible Nanocarriers embedded in Poloxamer 407 hydrogels as therapeutic formulations, Medicines. 6 (2018), https://doi.org/10.3390/medicines6010007.

[21] G. Vanti, D. Bani, M.C. Salvatici, M.C. Bergonzi, A.R. Bilia, Development and percutaneous permeation study of escinosomes, escin-based nanovesicles loaded with berberine chloride, Pharmaceutics. 11 (2019), https://doi.org/10.3390/pharmaceutics11120682.

[22] G. Vanti, M. Capizzi, L. di Cesare Mannelli, E. Lucarini, M.C. Bergonzi, C. Ghelardini, A.R. Bilia, Escinosomes: safe and successful Nanovesicles to deliver Andrographolide by a subcutaneous route in a mice model of Oxaliplatin-induced neuropathy, Pharmaceutics. 14 (2022), https://doi.org/10.3390/pharmaceutics14030493.

[23] S.H. Butler, F. Godefroy, J.M. Besson, J. Weil-Fugazza, A limited arthritic model for chronic pain studies in the rat, Pain. 48 (1992), https://doi.org/10.1016/0304-3959(92)90133-V.

[24] M. Maresca, L. Micheli, L. Cinci, A.R. Bilia, C. Ghelardini, L. di Cesare Mannelli, Pain relieving and protective effects of Astragalus hydroalcoholic extract in rat arthritis models, J. Pharm. Pharmacol. 69 (2017), https://doi.org/10.1111/jphp.12828.

[25] P. Guo, J. Huang, Y. Zhao, C.R. Martin, R.N. Zare, M.A. Moses, Nanomaterial preparation by extrusion through Nanoporous membranes, Small. 14 (2018), https://doi.org/10.1002/smll.201703493.

[26] H. Zhang, Thin-film hydration followed by extrusion method for liposome preparation, Methods Mol. Biol. (2017), https://doi.org/10.1007/978-1-4939-6591-5_2.

[27] R. Bnyan, I. Khan, T. Ehtezazi, I. Saleem, S. Gordon, F. O'Neill, M. Roberts, Surfactant effects on lipid-based vesicles properties, J. Pharm. Sci. 107 (2018), https://doi.org/10.1016/j.xphs.2018.01.005.

[28] A.C. Biondi, E.A. Disalvo, Effect of glycerol on the interfacial properties of dipalmitoylphosphatidylcholine liposomes as measured with merocyanine 540, BBA - Biomembran. 1028 (1990), https://doi.org/10.1016/0005-2736(90)90263-N.

[29] T. Kaneko, H. Sagitani, Formation of homogeneous liposomes with high trapping efficiency by the surface chemical method, Colloids Surf. A Physicochem. Eng. Asp. 69 (1992), https://doi.org/10.1016/0166-6622(92)80223-O.

[30] G. Vanti, E.-M. Tomou, D. Stojković, A. Ćirić, A.R. Bilia, H. Skaltsa, Nanovesicles loaded with origanum onites and satureja thymbra essential oils and their activity against food-borne pathogens and spoilage microorganisms, Molecules. 26 (2021), https://doi.org/10.3390/molecules26082124.

[31] H. Xia, H. Jin, Y. Cheng, Z. Cheng, Y. Xu, The controlled release and anti-inflammatory activity of a Tetramethylpyrazine-loaded thermosensitive Poloxamer hydrogel, Pharm. Res. 36 (2019), https://doi.org/10.1007/s11095-019-2580-0.

[32] M. Srivastava, K. Kohli, M. Ali, Formulation development of novel in situ nanoemulgel (NEG) of ketoprofen for the treatment of periodontitis, Drug Deliv. 23 (2016), https://doi.org/10.3109/10717544.2014.907842.

[33] S. Bhattacharjee, In relation to the following article "DLS and zeta potential — what they are and what they are not?" journal of controlled release, 2016, 235, 337–351, J. Control. Release 238 (2016), https://doi.org/10.1016/j.jconrel.2016.07.002.
[34] F. Varenne, J. Botton, C. Merlet, H. Hillaireau, F.X. Legrand, G. Barratt, C. Vauthier, Size of monodispersed nanomaterials evaluated by dynamic light scattering: protocol validated for measurements of 60 and 203 nm diameter nanomaterials is now extended to 100 and 400 nm, Int. J. Pharm. 515 (2016), https://doi.org/10.1016/j.ijpharm.2016.10.016.
[35] ISO 22412, Particle size analysis-Dynamic light scattering (DLS), 2008.
[36] G. Vanti, L.D.C. Mannelli, L. Micheli, L. Cinci, L. Grifoni, M.C. Bergonzi, C. Ghelardini, A.R. Bilia, The anti-arthritic efficacy of khellin loaded in ascorbyl decanoate nanovesicles after an intra-articular administration, Pharmaceutics. 13 (2021), https://doi.org/10.3390/pharmaceutics13081275.
[37] E.L. Bortel, B. Charbonnier, R. Heuberger, Development of a synthetic synovial fluid for tribological testing, Lubricants. 3 (2015), https://doi.org/10.3390/lubricants3040664.
[38] E.G. Yarmola, Y. Shah, D.P. Arnold, J. Dobson, K.D. Allen, Magnetic capture of a molecular biomarker from synovial fluid in a rat model of knee osteoarthritis, Ann. Biomed. Eng. 44 (2016), https://doi.org/10.1007/s10439-015-1371-y.
[39] N. Nafee, M. Zewail, N. Boraie, Alendronate-loaded, biodegradable smart hydrogel: a promising injectable depot formulation for osteoporosis, J. Drug Target. 26 (2018), https://doi.org/10.1080/1061186X.2017.1390670.
[40] G. Vanti, M. Wang, M.C. Bergonzi, L. Zhidong, A.R. Bilia, Hydroxypropyl methylcellulose hydrogel of berberine chloride-loaded escinosomes: dermal absorption and biocompatibility, Int. J. Biol. Macromol. 164 (2020), https://doi.org/10.1016/j.ijbiomac.2020.07.129.
[41] Y. Liu, Y. Zhu, G. Wei, W. Lu, Effect of carrageenan on poloxamer-based in situ gel for vaginal use: improved in vitro and in vivo sustained-release properties, Eur. J. Pharm. Sci. 37 (2009) 306–312, https://doi.org/10.1016/j.ejps.2009.02.022.
[42] L. Bai, F. Lei, R. Luo, Q. Fei, Z. Zheng, N. He, S. Gui, Development of a thermosensitive in-situ gel formulations of vancomycin hydrochloride: design, preparation, in vitro and in vivo evaluation, J. Pharm. Sci. 111 (2022) 2552–2561, https://doi.org/10.1016/j.xphs.2022.04.011.
[43] M. Sharma, K. Chandramouli, L. Curley, B. Pontre, K. Reilly, J. Munro, A. Hill, S. Young, D. Svirskis, In vitro and ex vivo characterisation of an in situ gelling formulation for sustained lidocaine release with potential use following knee arthroplasty, Drug Deliv. Transl. Res. 8 (2018), https://doi.org/10.1007/s13346-018-0492-x.
[44] L. Micheli, M. Bozdag, O. Akgul, F. Carta, C. Guccione, M.C. Bergonzi, A.R. Bilia, L. Cinci, E. Lucarini, C. Parisio, C.T. Supuran, C. Ghelardini, L. di Cesare Mannelli, Pain relieving effect of-NSAIDS-CAIs hybrid molecules: systemic and intra-articular treatments against rheumatoid arthritis, Int. J. Mol. Sci. 20 (2019), https://doi.org/10.3390/ijms20081923.
[45] G.E. Leighton, R.E. Rodriguez, R.G. Hill, J. Hughes, κ-Opioid agonists produce antinociception after i.v. and i.c.v. but not intrathecal administration in the rat, Br. J. Pharmacol. 93 (1988), https://doi.org/10.1111/j.1476-5381.1988.tb10310.x.
[46] S.E. Bove, S.L. Calcaterra, R.M. Brooker, C.M. Huber, R.E. Guzman, P.L. Juneau, D. J. Schrier, K.S. Kilgore, Weight bearing as a measure of disease progression and efficacy of anti-inflammatory compounds in a model of monosodium iodoacetate-induced osteoarthritis, Osteoarthr. Cartil. 11 (2003), https://doi.org/10.1016/S1063-4584(03)00163-8.
[47] M. Sakurai, N. Egashira, T. Kawashiri, T. Yano, H. Ikesue, R. Oishi, Oxaliplatin-induced neuropathy in the rat: involvement of oxalate in cold hyperalgesia but not mechanical allodynia, Pain. 147 (2009), https://doi.org/10.1016/j.pain.2009.09.003.
[48] Y. Ding, J. Li, Q. Lai, J.A. Rafols, X. Luan, J. Clark, F.G. Diaz, Motor balance and coordination training enhances functional outcome in rat with transient middle cerebral artery occlusion, Neuroscience. 123 (2004), https://doi.org/10.1016/j.neuroscience.2003.08.031.
[49] L. Micheli, C. Ghelardini, E. Lucarini, C. Parisio, E. Trallori, L. Cinci, L. di Cesare Mannelli, Intra-articular mucilages: behavioural and histological evaluations for a new model of articular pain, J. Pharm. Pharmacol. 71 (2019), https://doi.org/10.1111/jphp.13078.
[50] U. Snekhalatha, M. Anburajan, B. Venkatraman, M. Menaka, Evaluation of complete Freund's adjuvant-induced arthritis in a Wistar rat model: comparison of thermography and histopathology, Z. Rheumatol. 72 (2013), https://doi.org/10.1007/s00393-012-1083-8.
[51] H. Maghsoudi, J. Hallajzadeh, M. Rezaeipour, Evaluation of the effect of polyphenol of escin compared with ibuprofen and dexamethasone in synoviocyte model for osteoarthritis: an in vitro study, Clin. Rheumatol. 37 (2018), https://doi.org/10.1007/s10067-018-4097-z.
[52] L. Zhang, Y. Huang, C. Wu, Y. Du, P. Li, M. Wang, X. Wang, Y. Wang, Y. Hao, T. Wang, B. Fan, Z. Gao, F. Fu, Network pharmacology based research on the combination mechanism between escin and low dose glucocorticoids in anti-rheumatoid arthritis, Front. Pharmacol. 10 (2019), https://doi.org/10.3389/fphar.2019.00280.
[53] Y. Du, Y. Song, L. Zhang, M. Zhang, F. Fu, Combined treatment with low dose prednisone and escin improves the anti-arthritic effect in experimental arthritis, Int. Immunopharmacol. 31 (2016), https://doi.org/10.1016/j.intimp.2016.01.006.
[54] M.K. Kosinska, T.E. Ludwig, G. Liebisch, R. Zhang, H.C. Siebert, J. Wilhelm, U. Kaesser, R.B. Dettmeyer, H. Klein, B. Ishaque, M. Rickert, G. Schmitz, T. A. Schmidt, J. Steinmeyer, Articular joint lubricants during osteoarthritis and rheumatoid arthritis display altered levels and molecular species, PLoS One 10 (2015), https://doi.org/10.1371/journal.pone.0125192.
[55] M.L. Kang, G. il Im, Drug delivery systems for intra-articular treatment of osteoarthritis, Expert Opin. Drug Deliv. 11 (2014), https://doi.org/10.1517/17425247.2014.867325.
[56] M. Zhang, W. Hu, C. Cai, Y. Wu, J. Li, S. Dong, Advanced application of stimuli-responsive drug delivery system for inflammatory arthritis treatment, Mater Today Bio. 14 (2022), https://doi.org/10.1016/j.mtbio.2022.100223.
[57] M.L. Kang, G. Il Im, Drug delivery systems for intra-articular treatment of osteoarthritis, Expert Opin. Drug Deliv. 11 (2014), https://doi.org/10.1517/17425247.2014.867325.
[58] M. Rahman, S. Beg, F. Anwar, V. Kumar, R. Ubale, R.T. Addo, R. Ali, S. Akhter, Liposome-based nanomedicine therapeutics for rheumatoid arthritis, Crit. Rev. Ther. Drug Carrier Syst. 34 (2017), https://doi.org/10.1615/CritRevTherDrugCarrierSyst.2017016067.
[59] X. Li, B. Dai, J. Guo, L. Zheng, Q. Guo, J. Peng, J. Xu, L. Qin, Nanoparticle–cartilage interaction: pathology-based intra-articular drug delivery for osteoarthritis therapy, Nano Lett. 13 (2021), https://doi.org/10.1007/s40820-021-00670-y.
[60] M. Rahman, G. Sharma, K. Thakur, F. Anwar, O. Katare, V. Goni, V. Kumar, M. Zamzami, S. Akhter, Emerging advances in nanomedicine as a nanoscale pharmacotherapy in rheumatoid arthritis: state of the art, Curr. Top. Med. Chem. 17 (2016), https://doi.org/10.2174/1568026616666160530152354.
[61] H. Abdeltawab, D. Svirskis, M. Sharma, Formulation strategies to modulate drug release from poloxamer based in situ gelling systems, Expert Opin. Drug Deliv. 17 (2020), https://doi.org/10.1080/17425247.2020.1731469.
[62] Q. Li, J. Cao, Z. Li, X. Chu, Cubic liquid crystalline gels based on glycerol Monooleate for intra-articular injection, AAPS PharmSciTech 19 (2018), https://doi.org/10.1208/s12249-017-0894-y.
[63] M. Zewail, N. Nafee, M.W. Helmy, N. Boraie, Synergistic and receptor-mediated targeting of arthritic joints via intra-articular injectable smart hydrogels containing leflunomide-loaded lipid nanocarriers, Drug Deliv. Transl. Res. 11 (2021), https://doi.org/10.1007/s13346-021-00992-9.
[64] C. Shinde, M.P. Venkatesh, T. Pramod Kumar, D.R. Pai, Nanostructured lipid carrier-based smart gel: a delivery platform for intra-articular therapeutics, Autoimmunity. 54 (2021), https://doi.org/10.1080/08916934.2020.1846184.
[65] R.P. Watt, H. Khatri, A.R.G. Dibble, Injectability as a function of viscosity and dosing materials for subcutaneous administration, Int. J. Pharm. 554 (2019), https://doi.org/10.1016/j.ijpharm.2018.11.012.
[66] N. Yin, X. Guo, R. Sun, H. Liu, L. Tang, J. Gou, T. Yin, H. He, Y. Zhang, X. Tang, Intra-articular injection of indomethacin-methotrexate: in situ hydrogel for the synergistic treatment of rheumatoid arthritis, J. Mater. Chem. B 8 (2020), https://doi.org/10.1039/c9tb01795j.
[67] B. Küçüktürkmen, U.C. Öz, A. Bozkir, *In situ* hydrogel formulation for intra-articular application of diclofenac sodium-loaded polymeric nanoparticles, Turk J. Pharm.Sci. 14 (2017), https://doi.org/10.4274/tjps.84803.
[68] T. Zhang, S. Chen, H. Dou, Q. Liu, G. Shu, J. Lin, W. Zhang, G. Peng, Z. Zhong, H. Fu, Novel glucosamine-loaded thermosensitive hydrogels based on poloxamers for osteoarthritis therapy by intra-articular injection, Mater. Sci. Eng. C 118 (2021), https://doi.org/10.1016/j.msec.2020.111352.
[69] S. More, A. Kotiya, A. Kotia, S.K. Ghosh, L.A. Spyrou, I.E. Sarris, Rheological properties of synovial fluid due to viscosupplements: a review for osteoarthritis remedy, Comput. Methods Prog. Biomed. 196 (2020), https://doi.org/10.1016/j.cmpb.2020.105644.
[70] A.S. Hanafy, S.O. El-Ganainy, Thermoresponsive Hyalomer intra-articular hydrogels improve monoiodoacetate-induced osteoarthritis in rats, Int. J. Pharm. 573 (2020), https://doi.org/10.1016/j.ijpharm.2019.118859.
[71] X. Qi, X. Qin, R. Yang, J. Qin, W. Li, K. Luan, Z. Wu, L. Song, Intra-articular Administration of Chitosan Thermosensitive in situ hydrogels combined with diclofenac sodium-loaded alginate microspheres, J. Pharm. Sci. 105 (2016), https://doi.org/10.1016/j.xphs.2015.11.019.
[72] M.C. Cristiano, A. Mancuso, E. Giuliano, D. Cosco, D. Paolino, M. Fresta, Etogel for intra-articular drug delivery: a new challenge for joint diseases treatment, J. Funct. Biomater. 12 (2021), https://doi.org/10.3390/JFB12020034.
[73] C. Larsen, J. Østergaard, S.W. Larsen, H. Jensen, S. Jacobsen, C. Lindegaard, P. H. Andersen, Intra-articular depot formulation principles: role in the management of postoperative pain and arthritic disorders, J. Pharm. Sci. 97 (2008), https://doi.org/10.1002/jps.21346.
[74] I. Ott, R. Gust, Stability, protein binding and thiol interaction studies on [2-acetoxy-(2-propynyl)benzoate]hexacarbonyldicobalt, BioMetals. 18 (2005), https://doi.org/10.1007/s10534-004-6252-z.
[75] J. Paik, S.T. Duggan, S.J. Keam, Triamcinolone Acetonide extended-release: a review in osteoarthritis pain of the knee, Drugs. 79 (2019), https://doi.org/10.1007/s40265-019-01083-3.
[76] P.C. Taylor, A. Moore, R. Vasilescu, J. Alvir, M. Tarallo, A structured literature review of the burden of illness and unmet needs in patients with rheumatoid arthritis: a current perspective, Rheumatol. Int. 36 (2016), https://doi.org/10.1007/s00296-015-3415-x.
[77] L. vande Walle, N. van Opdenbosch, P. Jacques, A. Fossoul, E. Verheugen, P. Vogel, R. Beyaert, D. Elewaut, T.D. Kanneganti, G. van Loo, M. Lamkanfi, Negative regulation of the NLRP3 inflammasome by A20 protects against arthritis, Nature. 512 (2014), https://doi.org/10.1038/nature13322.
[78] W. Park, D.H. Yoo, C.H. Suh, S.C. Shim, S.J. Lee, S.Y. Lee, J.H. Park, Y.M. Bae, S. H. Kim, S.G. Lee, AB0433 Meta-analysis of the safety data between infliximab biosimilar (CT-P13) and innovator infliximab in rheumatoid arthritis and ankylosing spondylitis: table 1, Ann. Rheum. Dis. 74 (2015), https://doi.org/10.1136/annrheumdis-2015-eular.4462.

[79] H.E. Vonkeman, M.A.F.J. van de Laar, Nonsteroidal anti-inflammatory drugs: adverse effects and their prevention, Semin. Arthritis Rheum. 39 (2010), https://doi.org/10.1016/j.semarthrit.2008.08.001.
[80] G.N. Chandler, V. Wright, Deleterious effect of intra-articular hydrocortisone, Lancet 272 (1958), https://doi.org/10.1016/S0140-6736(58)92262-1.
[81] J.G. McGarry, Z.J. Daruwalla, The efficacy, accuracy and complications of corticosteroid injections of the knee joint, knee surgery, sports traumatology, Arthroscopy. 19 (2011), https://doi.org/10.1007/s00167-010-1380-1.
[82] A.A. Abdin, M.S. Abd El-Halim, S.E. Hedeya, A.A.E. El-Saadany, Effect of atorvastatin with or without prednisolone on Freund's adjuvant induced-arthritis in rats, Eur. J. Pharmacol. 676 (2012), https://doi.org/10.1016/j.ejphar.2011.11.052.
[83] N. Schuelert, J.J. McDougall, Grading of monosodium iodoacetate-induced osteoarthritis reveals a concentration-dependent sensitization of nociceptors in the knee joint of the rat, Neurosci. Lett. 465 (2009), https://doi.org/10.1016/j.neulet.2009.08.063.
[84] L. Gallelli, Escin: a review of its anti-edematous, antiinflammatory, and venotonic properties, Drug Des. Devel. Ther. 13 (2019), https://doi.org/10.2147/DDDT.S207720.
[85] C.T. Supuran, Multitargeting approaches involving carbonic anhydrase inhibitors: hybrid drugs against a variety of disorders, J. Enzyme Inhib. Med. Chem. 36 (2021), https://doi.org/10.1080/14756366.2021.1945049.
[86] J.C. McGrath, E. Lilley, Implementing guidelines on reporting research using animals (ARRIVE etc.): new requirements for publication in BJP, Br. J. Pharmacol. 172 (2015), https://doi.org/10.1111/bph.12955.